Possibility Generalized Labeled Multi-Bernoulli Filter For Multi-Target Tracking Under Epistemic Uncertainty

Han Cai
Beijing Institute of Technology, Beijing 100081, China

Jeremie Houssineau
University of Warwick, Coventry, CV4 7AL UK

Brandon A Jones, Member, IEEE
The University of Texas at Austin, Austin, Texas 78712, USA

Moriba Jah, Senior Member, IEEE
The University of Texas at Austin, Austin, Texas 78712, USA

Jingrui Zhang
Beijing Institute of Technology, Beijing 100081, China

Abstract— **This paper presents a flexible modeling framework for multi-target tracking based on the theory of Outer Probability Measures (OPMs). The notion of labeled uncertain finite set is introduced and utilized as the basis to derive a possibilistic analog of the δ-Generalized Labeled Multi-Bernoulli (δ-GLMB) filter, in which the uncertainty in the multi-target system is represented by possibility functions instead of probability distributions. The proposed method inherits the capability of the standard probabilistic δ-GLMB filter to yield joint state, number, and trajectory estimates of multiple appearing and disappearing targets. Beyond that, it is capable to account for epistemic uncertainty due to ignorance or partial knowledge regarding the multi-target system, e.g., the absence of complete information on dynamical model parameters (e.g., probability of detection, birth) and initial number and state of newborn targets. The features of the developed filter are demonstrated using two simulated scenarios.**

Index Terms— **Generalized labeled multi-Bernoulli filter, epistemic uncertainty, multi-target tracking.**

H. Cai is with the Department of Aerospace Engineering, Beijing Institute of Technology, Beijing 100081, China (e-mail: caihanspace@gmail.com). J. Houssineau is with the Department of Statistics, University of Warwick, Coventry, CV4 7AL UK (e-mail: jeremie.houssineau@warwick.ac.uk). B.A. Jones is with the Department of Aerospace Engineering and Engineering Mechanics, The University of Texas at Austin, Austin, Texas 78712, USA (e-mail: brandon.jones@utexas.edu). M. Jah is with the Department of Aerospace Engineering and Engineering Mechanics, The University of Texas at Austin, Austin, Texas 78712, USA (e-mail: moriba@utexas.edu) J. Zhang is with the Department of Aerospace Engineering, Beijing Institute of Technology, Beijing 100081, China (e-mail: zhangjingrui@bit.edu.cn)

Color versions of one or more of the figures in this article are available online at http://ieeexplore.ieee.org.

0018-9251 © 2022 IEEE

I. INTRODUCTION

THE Multi-Target Tracking (MTT) problem is to jointly estimate the number, state, and individual trajectory of targets based on a sequence of measurements, where the number of targets may be time varying due to possible birth and death events. The major challenge in this process is to resolve various sources of uncertainty stemming from target-to-measurement association, false alarm, and missed detection. Over the years numerous multi-target tracking algorithms have been developed based on the multi-target Bayes filter, and three of the major methodologies are Multiple Hypothesis Tracking (MHT) [1], Joint Probabilistic Data Association (JPDA) [2], and Random Finite Set (RFS) [3].

The RFS approach is the latest solution to the MTT problem. It provides a general systematic treatment of multi-target systems by modeling the multi-target state as finite set valued random variables, which enables the derivation of multi-target filters based on Bayes' theorem. Several realizations of RFS filters have been developed, including the Probability Hypothesis Density (PHD) [4], Cardinalized Probability Hypothesis Density (CPHD) [5], and Multi-Bernoulli (MB) [6] filters. However, the above methods cannot provide trajectory-related information, which are of particular interest in many applications, e.g., space surveillance. To cope with this issue, Vo. et al [7, 8] further developed the Generalized Labeled Multi-Bernoulli (GLMB) filter based on the notion of labeled RFS. In the GLMB filter, a unique label is assigned to each target for identity maintenance, and the corresponding trajectory can be reconstructed by extracting the sequence of estimates with the same label. Beyond that, the GLMB filter outperforms the PHD, CPHD and MB filters in terms of state estimation accuracy. Efficient approximations of the GLMB filter, e.g., the Labeled Multi-Bernoulli (LMB) filter [9] and Marginalized GLMB filter [10], further facilitate the application of labeled RFS filters in several disciplines, e.g. track before detect [11], sensor control [12, 13, 14], and information fusion [15, 16].

In the GLMB method, the recursive estimation of the filtering density of the multi-target state relies on the framework of the Bayes multi-target filter. In the typical Bayes multi-target filter, all uncertain components in the multi-target system are modelled as aleatoric, and they must be characterized by a probability distribution based on the assumption that one possess complete knowledge or sufficient statistical information of the system. For instance, the newborn targets and false alarms are usually assumed as uniformly or Poisson distributed within the sensor Field-of-View (FOV). However, in many realistic applications, the exact knowledge concerning the birth model and detection profile may not be available for analysis. This kind of uncertainty that results from the lack of information is referred to as epistemic uncertainty. As opposed to the inherent randomness of the system, epistemic uncertainty is reducible if we can keep collecting and processing information to learn all aspect of the system. Modeling epistemic uncertainty using a probabilistic model may result in ill-adapted representation [17]. The mismatches between the assumed model and the reality may result in performance degradation of the filter, such as erroneous state and cardinality estimations [18]. Several versions of RFS filters, including CPHD [5] and GLMB [19, 20] filter, have been proposed to adaptively estimate unknown detection profile and clutter rate while filtering. However, these methods are less effective when the detection profile and clutter background evolve rapidly compared to the measurement-update rate.

The recently developed Outer Probability Measures (OPMs) framework [21] yield an alternative representation of limited information of a complex system. Closed-form filtering solutions based on OPMs have been derived for a recursive so-called uninformative prior Bayesian estimation [22] for enhanced robustness in the absence of precise measurements or dynamic model assumptions. Ref. [23] explores the concept of Uncertain Finite Set (UFS) by replacing the random variables in a RFS with uncertain variables, and the possibility Bernoulli filter on the basis of UFS has been developed to accommodate the presence of partial knowledge on the model and filtering parameters. In [18], a uncertain finite set is also referred to as uncertain counting measure, which is employed to model the multi-target tracking system and develop a possibilistic version of the PHD filter. The possibility PHD filter provides significant modeling versatility for multi-target systems and enables an appropriate representation of imperfect information about the number and state of newborn targets. However, similar to the PHD filter, the possibilistic analog cannot provide trajectory information. In addition, directly estimating the number of targets is not possible in this method.

In this paper, a robust multi-target tracker is developed to provide joint state, number, and trajectory estimates with very little information about some aspects of the underlying processes, e.g., birth process and detection profiles. The proposed approach allows to represent uncertainty in parameters without necessarily using additional levels of modelling (such as hyperparameters or false-alarm generators employed in Refs. [5, 19]). To this end, we exploits the notion of labeled UFS by adapting the labeled RFS approach to the OPM framework. The GLMB UFS is introduced as the form of weighted maximum of multi-target exponentials, which also satisfies the property of conjugate priors that are closed under the Chapman-Kolmogorov equation. The predict-update recursion of the GLMB UFS is shown to take the same form as the standard version with integrals replaced by supremums. On top of that, the developed possibility δ-GLMB filter can handle the MTT problem in the situation of ignorance or partial knowledge in the MTT problem. The performance of the developed method is verified by comparing with the standard δ-GLMB filter using two simulated MTT scenarios.

The rest of the paper is organized as follows. Sec. II briefly reviews the mathematical foundation of OPMs and possibilistic Bayesian multi-target inference. The theory of labeled UFS is introduced in Sec. III, followed by the definition of the GLMB UFS and recursion given in Sec. V. Sec.VI elaborates the implementation of the possibility δ-GLMB filter. The simulation results are presented in Sec. VII and concluding remarks are given in Sec. VIII.

II. Background

In this section, the mathematical definition of OPMs will be first introduced, followed by a description of the multi-target filter based on the possibilistic Bayesian inference.

A. Outer Probability Measures and Possibility Functions

An outer probability measure is essentially a set function $\bar{P}$ defined on the state space $\mathbb{X}$, and $\bar{P}(A) \in [0,1]$ indicates the credibility of the event $X \in A$ for all subsets A of $\mathbb{X}$, where X is referred to as uncertain variable as opposed to a random variable to represent an uncertain system. In addition, $\bar{P}$ satisfies the following properties [21]:

$$\begin{cases} \bar{P}(\emptyset) = 0 \\ \bar{P}(\mathbb{X}) = 1 \\ \bar{P}(A) \leq \bar{P}(B), \quad A \subseteq B \\ \bar{P}\left(\bigcup_{i=1}^{\infty} A_i\right) \leq \sum_{i=1}^{\infty} \bar{P}(A_i), \quad \forall A_i \subseteq \mathbb{X}. \end{cases}$$

OPMs are distinct from probability measure because they are non-additive. Given two subsets A and B of $\mathbb{X}$, the probability of the two events $X \in A$ and $X \in B$ sums to one: $P(A) + P(B) = 1$, while OPMs instead consider $\bar{P}(A \cup B) \leq \bar{P}(A) + \bar{P}(B)$. Due to the concept of non-additivity, OPMs provide additional flexibility for modeling ignorance [21]. For instance, $\bar{P}(A) = 1$ and $\bar{P}(B) = a$ denote that the probability of $X \in A$ is unknown as we lack the evidence to discard any possibility of this event, and the probability of $X \in B$ is no more than a. This example indicates that an OPM $\bar{P}$ defines an upper bound for the underlying probability distributions. For $X \in A$, it follows that

$$1 - \bar{P}(\mathbb{X} \setminus A) \leq P(A) \leq \bar{P}(A),$$

where $\cdot\setminus\cdot$ denotes the set difference, and $\bar{P}(A)$ and $1-\bar{P}(\mathbb{X}\setminus A)$ are also respectively referred to as possibility measure and necessity measure in possibility theory [24]. As more information is available for analysis, the upper and lower bound in the above definition will converge to $P(A)$. In the extreme case of $1 - \bar{P}(\mathbb{X} \setminus A) = P(A) = \bar{P}(A)$, the analyst knows the probability of $X \in A$, meaning that there is no epistemic uncertainty left at that point.

This article has been accepted for publication in IEEE Transactions on Aerospace and Electronic Systems. This is the author's version which has not been fully edited and content may change prior to final publication. Citation information: DOI 10.1109/TAES.2022.3200022

We will focus on the class of OPMs, which are defined by a possibility function $f(x) \in [0,1]$ as follows

$$\bar{P}(A) = \sup_{x\in A} f(x).$$

A possibility function is normalized with maximum or supremum equals to one, i.e., $\max_{x\in\mathbb{X}} f(x) = 1$ or $\sup_{x\in\mathbb{X}} f(x) = 1$. Possibility functions can be related to fuzzy sets and belief functions as described in [25] and [26]. Given two uncertain variables x and y, then the marginal and posterior possibility functions are defined as

$$f(y) = \sup_{x\in\mathbb{X}} f(x,y), \;\; f(x|y) = \frac{f(x,y)}{f(y)},$$

where $f(x,y)$ is the joint possibility function that describes x and y. If x and y are said to be independently described, when $f(x,y) = f(x)f(y)$. There are various notions of conditioning and independence in possibility theory [27], we follow the route of *numerical* possibility theory for its strong connections with probability theory.

The simplest possibility function is called the indicator function, i.e., $f(x) = \mathbf{1}_A(x)$, which indicates $x \in A$ almost surely but no further information is available to describe the distribution of x within A. The indicator function has been applied in [28] to provide an "uninformative" initial orbital state of a space object.

Another commonly used possibility function is the Gaussian possibility function $f(x) = \bar{\mathcal{N}}(x;\mu,S)$, where

$$\bar{\mathcal{N}}(x;\mu,S) = \exp\Big(-\frac{1}{2}(x-\mu)^T S^{-1}(x-\mu)\Big),$$

for some $\mu \in \mathbb{R}^d$ and some $d\times d$ positive definite matrix S. In this paper, the μ and S are defined as possibilistic expected value and variance, respectively. The probabilistic mean in a Gaussian Probability Density Function (PDF) $p(x) = \mathcal{N}(x;\mu,S)$ represents a state that is statistically most likely, while the possibilistic expected value corresponds to the mode of the possibility function, indicating the value that we have least information to reject. In addition, the possibilistic variance describes the spread of the function. Unlike a Gaussian PDF, the Gaussian possibility function does not characterize the aleatory behavior, while it can be interpreted as a given shape of uncertainty or an upper bound of all underlying probability distributions.

A Gaussian Max-Mixture (GMM) possibility function takes the form of a weighted combination of Gaussian possibility functions. A GMM with N max-mixture components is defined by

$$f(x) = \max_{1\le i\le N} w_i\, \bar{\mathcal{N}}(x;\mu_i,S_i),$$

where $w_i \in [0,1]$ and $\max\limits_{1\le i\le N} w_i = 1$. The GMM is similar in formulation to a probabilistic Gaussian mixture model, e.g., $p(x) = \sum_{i=1}^N w_i p_i(x)$, $p_i(x) = \mathcal{N}(x;\mu_i,S_i)$, and $\sum_{i=1}^N w_i = 1$. The Gaussian mixture model suffices to approximate any smooth PDF with a specific nonzero amount of error using enough components [29]. Likewise, the GMM function can be cast as a universal approximation of any possibility function.

B. Possibility Bayes Multi-Target Filter

By replacing the notion of a random variable with the one of uncertain variable, the possibilistic analog of the standard Bayes multi-target filter is introduced in this section. The following notation are employed in the remainder of this paper. Single-target variables are denoted by lower-case letters (e.g., x, z), multi-target variables are represented by upper-case letters (e.g., X, Z), and the labeled states and distributions are denoted by bold-type symbols (e.g., $\boldsymbol{x}$, $\boldsymbol{X}$ and $\boldsymbol{\pi}$). The multi-target exponential is represented by $[f]^X = \prod_{x\in X} f(x)$, where $f^\emptyset = 1$. The black-board bold letters indicate spaces (e.g., the multi-target state space $\mathbb{X}$ and the measurement space $\mathbb{Z}$). The multi-target state and observations are upper case letters $X \in \mathcal{F}(\mathbb{X})$ and $Z \in \mathcal{F}(\mathbb{Z})$, respectively, where $\mathcal{F}(\mathbb{X})$ denotes all finite subset of $\mathbb{X}$, and $\mathcal{F}_n(\mathbb{X})$ denotes the collection of finite subsets of $\mathbb{X}$ with n elements.

Suppose the multi-target state at time t_{k-1} is an uncertain variable X_{k-1} on $\mathbb{X}$, all the available information about the number and multi-target state at time t_{k-1} is modeled by a possibility function $\pi_{k-1}(X_{k-1}|Z_{1:k-1})$, which is conditioned on the observation history $Z_{1:k-1}$. The multi-target prior at time t_k is the predicted possibility function $\pi_k(X_k|Z_{1:k-1})$ obtained based on the multi-target transition kernel $f_{k|k-1}(X_k|X_{k-1})$ using the following equation

$$\pi_k(X_k|Z_{1:k-1}) = \sup_{X\in\mathcal{F}(\mathbb{X})} \Big[f_{k|k-1}(X_k|X)\pi_{k-1}(X|Z_{1:k-1})\Big], \tag{1}$$

where the conditional possibility function $f_{k|k-1}(X_k|X)$ describes the transition of the target's state X_k given $X_{k-1} = X$.

The predicted possibility function $\pi_k(X_k|Z_{1:k-1})$ can then be updated by the information contained in the new observation Z_k based on Bayesian inference. Assuming the observation process is also modeled by a possibility function $g_k(Z_k|X_k)$ for observation Z_k, the posterior possibility function is expressed as

$$\pi_k(X_k|Z_{1:k}) = \frac{g_k(Z_k|X_k)\pi_k(X_k|Z_{1:k-1})}{\sup\limits_{X\in\mathcal{F}(\mathbb{X})} g_k(Z_k|X)\pi_k(X|Z_{1:k-1})}. \tag{2}$$

The prediction and update formulas can be seen as the possibilistic analog of the multi-target Chapman-Kolmogorov equation and the Bayes' update equation, respectively. The major difference is that the supremums are utilized to replace integrals, and the state transition function $f_{k|k-1}$ and the likelihood function g_k are represented by possibility functions instead of PDFs.

III. Labeled Uncertain Finite Set

This section first reviews the fundamental of UFS with a few examples in Sec. A, and then introduces the definition of labeled UFS and LMB UFS in Sec. B.

A. Uncertain Finite Set

1. *Concept of Uncertain Finite Set*

An UFS $X \in \mathcal{F}(\mathbb{X})$ is a finite set valued uncertain variable, where the number of points in X and the points themselves are uncertain. An UFS is completely described by its cardinality function and spatial distribution. The cardinality function of X is a discrete possibility function $f_c(n) = \bar{P}(|X| = n)$, and $\max_{n\geq 0} f_c(n) = 1$. The spatial distribution of X is a symmetric possibility function denoted by $f_n(x_1, \dots, x_n)$ with supremum equals one, i.e., $\sup_{x_1,\dots,x_n} f_n(x_1, \dots, x_n) = 1$. The possibility function of an UFS $X = \{x_1, \dots, x_n\}$ is defined by [23]

$$\pi(X) = f_c(n) f_n(x_1, \dots, x_n). \tag{3}$$

If the uncertain variables $x_1, \dots, x_n$ in an UFS X are independently described by the same possibility function $f(\cdot)$, then they are regarded as independently identically described (i.i.d.). The possibility function of the UFS X is expressed as

$$\pi(X) = f_c(|X|) \prod_{x\in X} f(x).$$

The supremum of the function $\pi(X)$ of an UFS X on $\mathbb{X}$ is referred to as *set supremum* in this paper, and the formal definition is given by

$$\sup_{X\subseteq\mathbb{X}} \pi(X) = \max_{n\geq 0} \left[\sup_{(x_1,\dots,x_n)\in\mathbb{X}^n} \pi(\{x_1, \dots, x_n\}) \right]. \tag{4}$$

The term within the max operator is the supremum of $n!$ permutations of $(x_1, \dots, x_n)$ in $\mathbb{X}^n$. This equation is in a form similar to Mahler's set integral equation for multi-target density functions [3]. The set integral takes the sum of the integrals for all the finite subsets X of $\mathbb{X}$, while (4) is determined by a single set of $(x_1, \dots, x_n)$ whose supremum is the maximum over n. Eq. (4) serves as one main base for deriving the GLMB recursion in Sec. V.

In [18], the concept of first-moment measure or intensity measure is extended to uncertain counting measure, which is defined as intensity measure. Following [18], the intensity measure of an UFS X is defined as

$$\bar{v}(x) = \max_{n\geq 0} \sup_{(x_1,\dots,x_n)\in\mathbb{X}^n} \pi(\{x\} \cup \{x_1, \dots, x_n\}). \tag{5}$$

The intensity measure of a RFS is the so-called Probability Hypothesis Density (PHD). The integral of the PHD over a region S gives the expected number of elements in S. However, the intensity measure cannot provide a cardinality information, and indeed, it yields the credibility that there is at least one point in S.

The following example is presented to provide insights into the principle of set supremum and intensity measure.

Example 1

Suppose the possibility function π of an UFS X is characterized by

$$\pi(\emptyset) = r_0^{(1)} r_0^{(2)} \tag{6a}$$

$$\pi(\{x\}) = \max\left\{ r_1^{(1)} r_0^{(2)} f^{(1)}(x), r_0^{(1)} r_1^{(2)} f^{(2)}(x) \right\} \tag{6b}$$

$$\pi(\{x_1, x_2\}) = r_1^{(1)} r_1^{(2)} \times \max\left\{ f^{(1)}(x_1) f^{(2)}(x_2), f^{(1)}(x_2) f^{(2)}(x_1) \right\} \tag{6c}$$

and by $\pi(X) = 0$ if $|X| > 2$, where $\max\{r_0^{(1)}, r_1^{(1)}\} = 1$, $\max\{r_0^{(2)}, r_1^{(2)}\} = 1$, and $f^{(1)}$ and $f^{(2)}$ are possibility functions, such that the supremum of each is equal to one. The set supremum of $\pi(X)$ is given by

$$\sup \pi(X) = \max\left\{ \pi(\emptyset),\ \sup_x \pi(\{x\}),\ \sup_{x_1,x_2} \pi(\{x_1, x_2\}) \right\}.$$

Substituting (6) into the above equation and simplifying the supremum of $f^{(1)}$ and $f^{(2)}$, we can easily conclude that $\sup \pi(X) = 1$. The intensity measure of $\pi(X)$ is given by

$$\bar{v}(y) = \max\left\{ r_1^{(1)} f^{(1)}(y), r_1^{(2)} f^{(2)}(y) \right\}.$$

This solution is obtained by substituting (6) into (5) and considering the supremum of possibility functions $f^{(1)}$ and $f^{(2)}$ is equal to one. Actually, the UFS X considered in this example is a multi-Bernoulli UFS, whose formal definition is given in the following section.

2. *Multi-Bernoulli Uncertain Finite Set*

The multi-Bernoulli UFS X is defined as the union of m independent Bernoulli UFS $X^{(i)}$, i.e., $X = \bigcup_{i=1}^m X^{(i)}$. A Bernoulli UFS X can be an empty set with possibility r_0 or a singleton with possibility r_1. Its possibility function $\pi(X)$ for a X on $\mathbb{X}$ is defined as [23]

$$\pi(X) = \begin{cases} r_0 & \text{if } X = \emptyset, \\ r_1 f(x) & \text{if } X = \{x\}. \end{cases} \tag{7}$$

Its cardinality is either 0 or 1. The maximum of a Bernoulli possibility function is equal one, i.e., $\max\{r_0, r_1 \sup_{x\in\mathbb{X}} f(x)\} = 1$, since $\sup_{x\in\mathbb{X}} f(x) = 1$ and $\max\{r_0, r_1\} = 1$. The definition of the multi-Bernoulli UFS is introduced below.

DEFINITION 1. *A multi-Bernoulli UFS is completely described by a parameter set* $\{(r_0^{(i)}, r_1^{(i)}, f^{(i)})\}_{i=1}^m$, *where* $\max\{r_0^{(i)}, r_1^{(i)}\} = 1$, *for* $i = 1, \dots, m$. *The possibility function of a multi-Bernoulli UFS for a set of non-empty* $X = \{x_1, \dots, x_n\}$ *is defined by*

$$\pi(X) = \prod_{i=1}^m r_0^{(i)} \max_{1\leq i_1\neq\dots\neq i_n\leq m} \prod_{j=1}^n \frac{r_1^{(i_j)}}{r_0^{(i_j)}} f^{(i_j)}(x_j). \tag{8}$$

The possibility function of a multi-Bernoulli UFS π *in the case of all the elements are empty set* $X^{(i)} = \emptyset$ *is* $\pi(\emptyset) = \prod_{i=1}^m r_0^{(i)}$.

The form of (8) is similar to the PDF of a multi-Bernoulli RFS [7], while the maximum replaces summation, and $r_0^{(i)}$ and $r_1^{(i)}$ are determined independently.

Based on the definition of UFS (3), the cardinality function of a multi-Bernoulli UFS can be obtained by $f_c(n) = \sup_{X \in \mathcal{F}_n(\mathbb{X})} \pi(X)$, i.e.,

$$f_c(n) = \prod_{i=1}^{m} r_0^{(i)} \max_{1 \le i_1 \ne \ldots \ne i_n \le m} \prod_{j=1}^{n} \frac{r_1^{(i_j)}}{r_0^{(i_j)}}. \tag{9}$$

We can easily conclude that $f_c(n)$ is a possibility function whose maximum is one since the maximum of (8) is equal to one (the proof is given in the Appendix).

B. Labeled Uncertain Finite Set

The fundamentals of the labeled UFS are similar to the probabilistic case [7], while the concepts and formulations presented in this section require a strict derivation for the sake of completeness.

1. *Fundamentals of Labeled Uncertain Finite Sets*

In order to distinguish the identity of each target, a unique label ℓ on a discrete labeled space $\mathbb{L}$ is assigned to each single-target state $x \in \mathbb{X}$, such that we obtain a labeled single-target state denoted by $\boldsymbol{x} = (x, \ell)$. Each label $\ell = (k, i)$ is uniquely determined by the birth time k of the target and the order i of birth at time k. The label of $\boldsymbol{x}$ can be retrieved using a projection function $\mathcal{L}((x, \ell)) = \ell$, where $\mathcal{L} : \mathbb{X} \times \mathbb{L} \to \mathbb{L}$.

A labeled UFS is defined as an UFS on $\mathbb{X} \times \mathbb{L}$ with state space $\mathbb{X}$ augmented by the label space $\mathbb{L}$. Each realization of a labeled UFS is a labeled multi-target state $\boldsymbol{X} = \{\boldsymbol{x}_1, \ldots, \boldsymbol{x}_n\}$ that has a distinct set of labels, i.e., $|\mathcal{L}(\boldsymbol{X})| = |\boldsymbol{X}|$. A distinct label indicator is denoted by $\Delta(\boldsymbol{X}) = \delta_{|\boldsymbol{X}|}(|\mathcal{L}(\boldsymbol{X})|)$, where the generalized Kronecker delta function $\delta_Y(X) = 1$ if and only if $X = Y$, and $\delta_Y(X) = 0$ otherwise.

Given a labeled UFS with possibility function $\boldsymbol{\pi}$, the UFS of a $\boldsymbol{X} = \{(x_1, \ell_1), \ldots, (x_n, \ell_n)\}$ is given by

$$\pi(\{x_1, \ldots, x_n\}) = \max_{(\ell_1, \ldots, \ell_n) \in \mathbb{L}^n} \boldsymbol{\pi}(\{(x_1, \ell_1), \ldots, (x_n, \ell_n)\}). \tag{10}$$

The unlabeled version is the projection from $\mathbb{X} \times \mathbb{L}$ into $\mathbb{X}$. The cardinality function of a labeled UFS should be the same as its unlabeled version. This is formalized by the following proposition.

PROPOSITION 1. *A labeled UFS has the same cardinality function as its unlabeled version. According to* (4) *and* (10)*, the set supremum of a function* $f : \mathbb{X} \times \mathbb{L} \to \mathbb{R}$ *is given by*

$$\sup_{\boldsymbol{X} \subseteq \mathbb{X} \times \mathbb{L}} \boldsymbol{\pi}(\boldsymbol{X}) = \max_{n \ge 0} \left[\max_{(\ell_1, \ldots, \ell_n) \in \mathbb{L}^n} \left[\sup_{\{x_1, \ldots, x_n\} \subseteq \mathbb{X}^n} \boldsymbol{\pi}\big(\{(x_1, \ell_1), \ldots, (x_n, \ell_n)\}\big) \right] \right]. \tag{11}$$

2. *Labeled Multi-Bernoulli Uncertain Finite Set*

Based on the definition of labeled UFS and multi-Bernoulli UFS, the labeled multi-Bernoulli UFS is introduced in this section. An LMB UFS $\boldsymbol{X}$ is defined on state space $\mathbb{X}$ and label space $\mathbb{L}$, and it can be completely represented by a parameter set $\{(r_0^{(\zeta)}, r_1^{(\zeta)}, f^{(\zeta)})\}_{\zeta \in \Omega}$, where ζ is some index defined in the index space Ω, and $\tau : \Omega \to \mathbb{L}$ is a $1-1$ mapping. If a Bernoulli component in an LMB yields a non-empty set, then a unique label $\tau(\zeta)$ is assigned to it. The possibility of a set of labeled states $\{(x_1, \ell_1), \ldots, (x_n, \ell_n)\}$ is given by

$$\boldsymbol{\pi}(\{(x_1, \ell_1), \ldots, (x_n, \ell_n)\}) = \delta_n(|\{\ell_1, \ldots, \ell_n\}|) \times \prod_{\zeta \in \Omega} r_0^{(\zeta)} \prod_{i=1}^{n} 1_{\tau(\Omega)}(\ell_i) \frac{r_1^{(\tau^{-1}(\ell_i))}}{r_0^{(\tau^{-1}(\ell_i))}} f^{(\tau^{-1}(\ell_i))}(x_i). \tag{12}$$

where $\boldsymbol{\pi}(\cdot)$ can be seen as the possibility function of an LMB RFS $\boldsymbol{X} = \{(x_1, \ell_1), \ldots, (x_n, \ell_n)\}$. For an empty set $\boldsymbol{X} = \emptyset$, the possibility function is $\boldsymbol{\pi}(\boldsymbol{X}) = \prod_{\zeta \in \Omega} r_0^{(\zeta)}$.

The unlabeled version of an LMB UFS is a multi-Bernoulli UFS, and this can be proven by substituting (12) into (10) and rearranging the terms within the maximum over the labels. Furthermore, according to (10), the maximum of LMB UFS is equal to its unlabeled version, indicating that the maximum of an LMB UFS is equal to one. In this paper, the formal definition of the LMB possibility function is given in the following definition.

DEFINITION 2. *The possibility function* $\boldsymbol{\pi}(\boldsymbol{X})$ *of an LMB UFS* $\boldsymbol{X}$ *is defined as*

$$\boldsymbol{\pi}(\boldsymbol{X}) = \Delta(\boldsymbol{X}) 1_{\tau(\Omega)}(\mathcal{L}(\boldsymbol{X})) \Big[\Phi(\boldsymbol{X}; \cdot) \Big]^{\Omega}, \tag{13}$$

where the indicator function $1_{\tau(\Omega)}(\mathcal{L}(\boldsymbol{X})) = 1$ *if and only if* $\mathcal{L}(\boldsymbol{X}) \in \tau(\Omega)$*. A component* $\Phi(\boldsymbol{X}; \zeta)$*,* $\zeta \in \Omega$ *within the exponential is given by*

$$\Phi(\boldsymbol{X}; \zeta) = \Big[\max_{(x, \ell) \in \boldsymbol{X}} \delta_{\tau(\zeta)}(\ell) r_1^{(\zeta)} f^{(\zeta)}(x) + \big(1 - 1_{\mathcal{L}(\boldsymbol{X})}(\tau(\zeta))\big) r_0^{(\zeta)} \Big].$$

where $\Phi(\boldsymbol{X}; \zeta) = r_1^{(\zeta)} f^{(\zeta)}(x)$ *if* $(x, \tau(\zeta)) \in \boldsymbol{X}$ *and* $\Phi(\boldsymbol{X}; \zeta) = r_0^{(\zeta)}$ *when* $\tau(\zeta) \notin \mathcal{L}(\boldsymbol{X})$.

In addition, (13) can be rearranged as the following alternative form

$$\boldsymbol{\pi}(\boldsymbol{X}) = \Delta(\boldsymbol{X}) w(\mathcal{L}(\boldsymbol{X})) f^{\boldsymbol{X}}, \tag{14}$$

where

$$w(L) = \prod_{i \in \mathbb{L}} r_0^{(i)} \prod_{\ell \in L} 1_{\mathbb{L}}(\ell) \frac{r_1^{(\ell)}}{r_0^{(\ell)}},$$
$$f(x, \ell) = f^{(\ell)}(x).$$

Eq. (14) closely resembles to the equation of LMB RFS except that each element in (14) is a Bernoulli UFS and the maximum of the weight $w(\cdot)$ is equal to one, i.e., $\max_{L \in \mathbb{L}} w(L) = 1$. It is shown in Sec. V that the LMB UFS can be seen as a special case of a GLMB UFS.

IV. Multi-Target Model

In this section, the possibilistic analog of the multi-target dynamical model and observation model are presented in Sec. A and B, respectively. It is possible to

This article has been accepted for publication in IEEE Transactions on Aerospace and Electronic Systems. This is the author's version which has not been fully edited and content may change prior to final publication. Citation information: DOI 10.1109/TAES.2022.3200022

utilize both the OPMs and the probability theory for modeling a MTT system in the case when we have a complete understanding of some aspects of the model but are ignorant of the rest [18]. For simplicity, this paper mainly focuses on the application of OPMs in modeling.

A. Dynamical Model

Let $\mathbb{L}_k$ denote the label space of all targets born at time k, the label space of all targets at time k is constructed by $\mathbb{L}_{0:k} = \mathbb{L}_{0:k-1} \cup \mathbb{L}_k$. In order to simplify notation, the time indices k and $k-1$ are omitted, and let $\mathbb{L} = \mathbb{L}_{0:k-1}$ denotes the label space at time $k-1$ and $\mathbb{B} = \mathbb{L}_k$ denotes the label space for newborn targets at time k, where $\mathbb{L}$ and $\mathbb{B}$ are disjoint. Then the label space at time k is denoted as $\mathbb{L}_+ = \mathbb{L} \cup \mathbb{B}$.

Given the multi-target state $\boldsymbol{X}$ at time $k-1$, each track (x, ℓ) either survives to time k with a possibility of survival $s_1(x, \ell)$ and generates a new single-target state (x_+, ℓ_+) with possibility $f(x_+|x, \ell)$, or disappears with a possibility $s_0(x, \ell)$. Note that $1 - s_0(x, \ell)$ and $s_1(x, \ell)$ can be interpreted as the lower and upper bound of the survival probability, and $\max\{s_0(x, \ell), s_1(x, \ell)\} = 1$. Track labels remain the same during the process of state transition.

Supposing the labels of the multi-target state $\boldsymbol{X}$ are distinct and the state transition of single-target state is independent, then the set $\boldsymbol{S}$ of states of the targets that survive to the next time is an LMB UFS that completely characterized by the parameter set $\{(s_0(\boldsymbol{x}), s_1(\boldsymbol{x}), f(\cdot|\boldsymbol{x})) : \boldsymbol{x} \in \boldsymbol{X}\}$, and $\boldsymbol{S}$ is described by the possibility function

$$\boldsymbol{\phi}_S(\boldsymbol{S}|\boldsymbol{X}) = \Delta(\boldsymbol{S})\Delta(\boldsymbol{X})1_{\mathcal{L}(\boldsymbol{X})}(\mathcal{L}(\boldsymbol{S}))\Big[\Phi(\boldsymbol{S};\cdot)\Big]^{\boldsymbol{X}},$$

where $\boldsymbol{\phi}_S(\boldsymbol{S}|\boldsymbol{X})$ is only defined when $\Delta\boldsymbol{X} = 1$, and

$$\Phi(\boldsymbol{S}; x, \ell) = \max_{(x_+, \ell_+) \in \boldsymbol{S}} \Big[\delta_\ell(\ell_+) s_1(x, \ell) f(x_+|, x, \ell) + (1 - 1_{\mathcal{L}(\boldsymbol{S})}(\ell)) s_0(x, \ell)\Big]. \tag{15}$$

The set $\boldsymbol{B}$ of new target birth with label space $\mathbb{B}$ is modeled by an LMB UFS with the parameter set $\{(r_{b,0}^{(\ell)}, r_{b,1}^{(\ell)}, f_B^{(\ell)})\}_{\ell=1}^{\mathbb{B}}$, where $r_{b,0}^{(\ell)}$ and $r_{b,1}^{(\ell)}$ denote the possibility of non-existence and existence of the newborn track ℓ, respectively, and $\max\{r_{b,0}^{(\ell)}, r_{b,1}^{(\ell)}\} = 1$. According to (14), the possibility function of a birth LMB UFS is given by

$$\boldsymbol{\phi}_B(\boldsymbol{B}) = \Delta(\boldsymbol{B}) w_B(\mathcal{L}(\boldsymbol{B}))[f_B]^{\boldsymbol{B}},$$

where

$$w_B(L) = \prod_{i \in \mathbb{B}} r_{b,0}^{(i)} \prod_{\ell \in L} 1_{\mathbb{B}}(\ell) \frac{r_{b,1}^{(\ell)}}{r_{b,0}^{(\ell)}},$$
$$f_B(x, \ell) = f_B^{(\ell)}(x).$$

$f_B(\cdot)$ is a possibility function that describes the distribution of a newborn state.

The multi-target state X at the next time is the superposition of the surviving objects and new born objects, i.e., $\boldsymbol{X}_+ = \boldsymbol{S} \cup \boldsymbol{B}$. As the birth and surviving objects are independent, the multi-target transition kernel is the product of the transition possibility function for surviving objects $\boldsymbol{X}_S = \boldsymbol{X}_+ \cap \mathbb{X} \times \mathbb{L}$ and new objects $\boldsymbol{X}_B = \boldsymbol{X}_+ - \mathbb{X} \times \mathbb{L}$, i.e.,

$$\boldsymbol{\phi}_+(\boldsymbol{X}_+|\boldsymbol{X}) = \boldsymbol{\phi}_S(\boldsymbol{X}_S|\boldsymbol{X})\boldsymbol{\phi}_B(\boldsymbol{X}_B).$$

B. Measurement Model

The measurements are modeled by an UFS $\boldsymbol{Z}$ with two independent components $Z = W \cup Y$, where the set W represents the detection from the targets and Y represents false observations. The set of detection W consists of detected points z and missed detection $\emptyset$. Specifically, a singe-target state $x \in X$ may be detected depending on the possibility of detection $d_1(\boldsymbol{x})$ and generates an observation $z \in W$ with the likelihood function $g(z|\boldsymbol{x})$. Alternatively, it may yield a missed detection $\emptyset$ with the possibility of detection failure $d_0(\boldsymbol{x})$. Hence, each $\boldsymbol{x}$ generates a Bernoulli UFS with the parameter set $(d_0(\boldsymbol{x}), d_1(\boldsymbol{x}), g(\cdot|\boldsymbol{x}))$. The set of detection W can then be represented as a multi-Bernoulli UFS, which is distributed according to the possibility function conditional on the multi-target state $\boldsymbol{X}$, i.e.,

$$\pi_D(W|\boldsymbol{X}) = \big\{d_0(\boldsymbol{x}), d_1(\boldsymbol{x}), g(\cdot|\boldsymbol{x})\big\}_{\boldsymbol{x} \in \boldsymbol{X}}(W). \tag{16}$$

The two functions $d_1(\boldsymbol{x})$ and $d_0(\boldsymbol{x})$ define the upper bound and lower bound for the probability of detection p_d via

$$1 - d_0(\boldsymbol{x}) \le p_d(\boldsymbol{x}) \le d_1(\boldsymbol{x}).$$

The probability of detection failure is totally deduced from the probability of detection p_d, while d_1 and d_0 are determined independently, and they verify that $\max\{d_1, d_0\} = 1$. The use of d_1 and d_0 properly reflects our ignorance regarding p_d. For instance, if it is not able to specify the exact value of p_d, but we can infer roughly that its value is greater than a. Then, we can set $d_1 = 1$ and $d_0 = 1 - a$ to describe all the limited information, and nothing more.

The set of false observations are modeled as an UFS Y, and its possibility function π_F is defined by [30]

$$\pi_F(Y) = \prod_{z \in Y} \kappa(z) = \kappa^Y, \tag{17}$$

where $\kappa(z)$ describes the possibility that z is a false alarm, and we have $\kappa(\varnothing) = 1$ to ensure $\kappa(\cdot)$ is a possibility function. Hence, $\pi_F(Y)$ is also a possibility function with supremum equals one: $\sup_{Y \subseteq \mathbb{Z}}(\pi_F(Y)) = 1$.

Given the possibility functions of detected measurements and false alarms, we define the multi-target likelihood function following [23], i.e.,

$$g(Z|\boldsymbol{X}) = \max_{W \subseteq Z} \Big[\pi_D(W|\boldsymbol{X})\pi_F(Z - W)\Big], \tag{18}$$

where the set difference $Z - W$ represents false alarms. Eq. (18) is slightly different from the standard labeled multi-target likelihood function as the use maximum instead of summation. The detailed equation of (18) in the GLMB form is given in the Appendix.

V. Possibility Generalized Labeled Multi-Bernoulli Filter

In this section, the GLMB UFS is introduced based on the theory of labeled UFS. Similar to the GLMB RFS, the possibility function of a GLMB UFS is conjugate with respect to the multi-object likelihood function, and it is closed under the multi-object Chapman-Kolmogorov equation. The results are similar to that of the probabilistic GLMB filter described in [7], and the derivations are given in the Appendix to justify the presented formulations.

A. Generalized Labeled Multi-Bernoulli Uncertain Finite Set

Definition 3. *A generalized labeled multi-Bernoulli UFS is defined on the state space $\mathbb{X}$ and label space $\mathbb{L}$ with possibility function given by*

$$\boldsymbol{\pi}(\boldsymbol{X}) = \Delta(\boldsymbol{X}) \max_{o\in\mathbb{O}} w^{(o)}(\mathcal{L}(\boldsymbol{X}))\left[f^{(o)}\right]^{\boldsymbol{X}}, \tag{19}$$

where $\mathbb{O}$ indicates a discrete index space, and

$$\max_{L\subseteq\mathbb{L}} \max_{o\in\mathbb{O}} w^{(o)}(L) = 1,$$
$$\sup_{x\in\mathbb{X}} f^{(o)}(x) = 1.$$

A GLMB UFS can be completely represented by the parameter set $\{w^{(o)}(I), f^{(o)}\}_{(I,o)\in\mathbb{L}\times\mathbb{O}}$.

The formulation of GLMB UFS is somewhat different from the GLMB RFS. Specifically, the GLMB RFS takes the form of a weighted sum of multi-target exponentials, and its density function is a probability distribution that integrates to one. The GLMB UFS is formulated as weighted maximum of multi-target exponentials, and the supremum of its possibility function is equal to one. In the case of only one element existing in the index space $\mathbb{O}$, the index o can be omitted and (19) is reduced to the LMB equation (14).

The cardinality function of a GLMB UFS $\boldsymbol{X}$ equals to n is given by

$$\begin{aligned} f_c(n) &= \sup_{(\boldsymbol{x}_1,\ldots,\boldsymbol{x}_n)\in(\mathbb{X}\times\mathbb{L})^n} \boldsymbol{\pi}(\boldsymbol{x}_1,\ldots,\boldsymbol{x}_n) \\ &= \max_{o\in\mathbb{O}} \max_{L\in\mathcal{F}_n(\mathbb{L})} w^{(o)}(L). \end{aligned} \tag{20}$$

It is clear that the cardinality function of a GLMB UFS is a possibility function.

$$\begin{aligned} \max_{n\geq 0} f_c(n) &= \max_{n\geq 0} \max_{L\in\mathcal{F}_n(\mathbb{L})} \max_{o\in\mathbb{O}} w^{(o)}(L) \\ &= \max_{L\subseteq\mathbb{L}} \max_{o\in\mathbb{O}} w^{(o)}(L) = 1. \end{aligned}$$

It is straightforward to derive that the supremum of the GLMB possibility function is equal to one, i.e.,

$$\begin{aligned} \sup_{\boldsymbol{X}\in\mathcal{F}(\mathbb{X}\times\mathbb{L})} \boldsymbol{\pi}(\boldsymbol{X}) &= \max_{n\geq 0} \sup_{(\boldsymbol{x}_1,\ldots,\boldsymbol{x}_n)\in(\mathbb{X}\times\mathbb{L})^n} \boldsymbol{\pi}(\boldsymbol{x}_1,\ldots,\boldsymbol{x}_n) \\ &= \max_{n\geq 0} f_c(n) = 1. \end{aligned} \tag{21}$$

The intensity measure of an unlabeled GLMB UFS can be derived by substituting the GLMB equation (19) into (5), i.e.,

$$\bar{v}(x) = \max_{o\in\mathbb{O}} \max_{\ell\in\mathbb{L}} \left[f^{(o)}(x,\ell) \max_{L\subseteq\mathbb{L}} 1_L(\ell) w^{(o)}(L)\right]. \tag{22}$$

The supremum of the intensity measure is given by

$$\begin{aligned} \sup_{x\in\mathbb{X}} \bar{v}(x) &= \max_{o\in\mathbb{O}} \max_{\ell\in\mathbb{L}} \max_{L\subseteq\mathbb{L}} 1_L(\ell) w^{(o)}(L) \\ &= \max_{n\geq 0} \max_{o\in\mathbb{O}} \max_{L\in\mathcal{F}_n(\mathbb{L})} w^{(o)}(L)\left[\max_{\ell\in\mathbb{L}} 1_L(\ell)\right] \\ &= \max_{n\geq 0} f_c(n) = 1. \end{aligned}$$

The last row is obtained by using (20) and $\max_{\ell\in\mathbb{L}} 1_L(\ell) = 1$. In contrast to the intensity measure or PHD of a GLMB RFS, the supremum of the GLMB intensity measure does not yield the expected number of targets, and it actually indicates that there is at least one point exists in the UFS. Nonetheless, it is still possible to estimate the cardinality of a GLMB UFS through $\bar{v}(\cdot)$. The intensity measure of each track ℓ can be extracted from (22), i.e.,

$$\bar{v}^{(\ell)}(x) = \max_{o\in\mathbb{O}} \max_{L\subseteq\mathbb{L}} 1_L(\ell) w^{(o)}(L) f^{(o)}(x,\ell).$$

As $\sup_{x\in\mathbb{X}} f^{(o)}(x,\ell) = 1$, the set supremum of $\bar{v}^{(\ell)}(\cdot)$ leads to the following form

$$\sup_{x\in\mathbb{X}} \bar{v}^{(\ell)}(x) = \max_{o\in\mathbb{O}} \max_{L\subseteq\mathbb{L}} 1_L(\ell) w^{(o)}(L).$$

In fact, the above equation indicates the maximum weight of all the hypotheses involving ℓ, and it can be interpreted as the possibility of existence of track ℓ. Hence, the cardinality of a GLMB UFS $\boldsymbol{X}$ can be estimated by assessing the possibility of existence of each track $\ell \in \mathcal{L}(\boldsymbol{X})$.

B. GLMB Uncertain Finite Set Recursion

1. Multi-Target Conjugate Prior

In Bayesian inference, the prior and posterior are regarded as conjugate distributions if they belong to the same category of distributions, and such a prior is called a conjugate prior. The feature of conjugacy plays a vital role in multi-target reasoning for deriving a closed-form solution of the posterior. The conjugacy of the GLMB UFS possibility function is introduced below.

Proposition 2. *If the multi-target prior is a GLMB function, then the multi-target posterior is also in a GLMB form under the multi-target likelihood function (18), i.e.,*

$$\boldsymbol{\pi}(Z|\boldsymbol{X}) = \Delta(\boldsymbol{X}) \max_{o\in\mathbb{O}} \max_{\theta\in\Theta} w^{(o,\theta)}(\mathcal{L}(\boldsymbol{X}))\left[f^{(o,\theta)}(\cdot|Z)\right]^{\boldsymbol{X}}, \tag{23}$$

where θ denotes an association map from the label space to observation indices, $\theta : \mathbb{L} \to \{0 : |Z|\}$, $\theta(\ell) = \theta(\ell') > 0$ indicates $\ell = \ell'$, and Θ is the space of association maps. The parameters of the posterior GLMB are given by

$$w^{(o,\theta)}(L) = \frac{\delta_{\theta^{-1}(\{0:|Z|\})}(L) w^{(o)}(L) \left[\eta_Z^{(o,\theta)}\right]^L}{\max\limits_{(o,\theta,J)\in\mathbb{O}\times\Theta\times\mathbb{L}} \delta_{\theta^{-1}(\{0:|Z|\})}(J) w^{(o)}(J) \left[\eta_Z^{(o,\theta)}\right]^J},$$

and by

$$f^{(o,\theta)}(x,\ell|Z) = \frac{f^{(o)}(x,\ell)\psi_Z(x,\ell;\theta)}{\eta_Z^{(o,\theta)}(\ell)},$$

$$\eta_Z^{(o,\theta)}(\ell) = \sup_{x\in\mathbb{X}} f^{(o)}(x,\ell)\psi_Z(x,\ell;\theta),$$

$$\psi_Z(x,\ell;\theta) = \begin{cases} \frac{d_1(x,\ell)g(z_{\theta(\ell)}|x,\ell)}{\kappa(z_{\theta(\ell)})} & \text{if } \theta(\ell) \neq 0, \\ d_0(x,\ell) & \text{if } \theta(\ell) = 0. \end{cases}$$

where $\theta^{-1}(\{0 : |Z|\})$ is to map the indices of measurements to the associated track labels.

2. Multi-Target Chapman-Kolmogorov Prediction

The GLMB UFS possibility function is closed under the multi-object Chapman-Kolmogorov equation regarding to the multi-object transition kernel.

PROPOSITION 3. *If the multi-target posterior is a GLMB function as the form of (19), then the multi-target prediction is also a GLMB with the following form*

$$\boldsymbol{\pi}_+(\boldsymbol{X}_+) = \Delta(\boldsymbol{X}_+) \max_{o\in\mathbb{O}} w_+^{(o)}(\mathcal{L}(\boldsymbol{X}_+)) \left[f_+^{(o)}\right]^{\boldsymbol{X}_+},$$

where

$$w_+^{(o)}(L) = w_B(L - \mathbb{L}) w_S^{(o)}(L \cap \mathbb{L}), \quad (24)$$

$$w_S^{(o)}(J) = \left[\eta_1^{(o)}\right]^J \max_{I\subseteq\mathbb{L}} 1_I(J) \left[\eta_0^{(o)}\right]^{I-J} w^{(o)}(I), \quad (25)$$

$$f_+^{(o)}(x,\ell) = 1_{\mathbb{L}}(\ell) f_S^{(o)}(x,\ell) + (1 - 1_{\mathbb{L}}(\ell)) f_B(x,\ell), \quad (26)$$

$$f_S^{(o)}(x,\ell) = \frac{\sup_{x'\in\mathbb{X}}[s_1(x',\ell)f(x|x',\ell)f^{(o)}(x',\ell)]}{\eta_1^{(o)}(\ell)}, \quad (27)$$

$$\eta_1^{(o)}(\ell) = \sup_{x\in\mathbb{X}} \sup_{x'\in\mathbb{X}} \left[s_1(x',\ell)f(x|x',\ell)f^{(o)}(x',\ell)\right], \quad (28)$$

$$\eta_0^{(o)}(\ell) = \sup_{x\in\mathbb{X}} s_0(x,\ell) f^{(o)}(x,\ell). \quad (29)$$

The equation of the weight $w_+^{(o)}(L)$ and possibility function $f_+^{(o)}(x,\ell)$ implies that the predicted GLMB is the combination of the newborn tracks and survival tracks. For an existing track ℓ, its possibility of survival and non-survival are represented by $\eta_1^{(o)}(\ell)$ and $\eta_0^{(o)}(\ell)$, respectively, and the normalisation constraint is $\max\{\eta_1^{(o)}(\ell), \eta_0^{(o)}(\ell)\} = 1$. The weight of a survival hypothesis J is proportional to the product of all the possibility of survival of tracks in J and the maximum of the prior weight over all label sets that contains J.

The propositions 2 and 3 can be seen as the possibilistic analog of the propositions 7 and respectively 8 in [7], and the proofs are given in the Appendix. These propositions indicate that for an initial prior described by a GLMB possibility function, the predicted and updated multi-target function is still in a GLMB form.

VI. Implementation of the Possibility GLMB Filter

In this section, a special form of the GLMB UFS, namely δ-GLMB UFS, is introduced as the basis for deriving an effective multi-target tracking algorithm. The joint prediction and update method is applied to the developed possibility δ-GLMB filter to improve the computational efficiency. The implementation of the filter for linear multi-target models is presented, followed by the introduction of the birth model and multi-target estimators. Compared with the probabilistic GLMB filter [7], the main differences in the implementation are the use of possibility functions to model imperfect information in the multi-target transition and measurement detection process, and the track extraction method which leverages the notion of *necessity* (also called *belief* in the context of Dempster-Shafer theory) is employed in multi-target estimation to select GLMB hypothesis with the maximum posterior weight.

A. δ-GLMB Uncertain Finite Set Recursion

DEFINITION 4. *A δ-generalized labeled multi-Bernoulli UFS is a special case of GLMB UFS, which is defined on the state space $\mathbb{X}$ and label space $\mathbb{L}$ with possibility function given by*

$$\boldsymbol{\pi}(\boldsymbol{X}) = \Delta(\boldsymbol{X}) \max_{(I,\xi)\in\mathcal{F}(\mathbb{L})\times\Xi} w^{(I,\xi)}\delta_I(\mathcal{L}(\boldsymbol{X})) \left[f^{(\xi)}\right]^{\boldsymbol{X}}, \quad (30)$$

where Ξ is a discrete space indicating the history of association maps in multi-target tracking scenarios. The coefficients in the above equation are related to (19) as follows

$$\mathcal{F}(\mathbb{L}) \times \Xi = \mathbb{O},$$

$$w^{(I,\xi)}\delta_I(L) = w^{(I,\xi)}(L) = w^{(o)}(L),$$

$$f^{(\xi)} = f^{(I,\xi)} = f^{(o)}.$$

A δ-GLMB UFS can be completely represented by the parameter set $\{w^{(I,\xi)}, f^{(\xi)}\}_{(I,\xi)\in\mathbb{L}\times\Xi}$.

The δ-GLMB UFS is a weighted maximum of multiple hypothesis. Each pair (I,ξ) defines a unique hypothesis indicating a set I of tracks with the history of track-to-measurement association ξ. The weight $w^{(I,\xi)}$ denotes the credibility of this hypothesis, and $f^{(\xi)}(\cdot,\ell)$ is the possibility function describing the state information of track ℓ. According to [7], the major advantage of δ-GLMB over GLMB lies in the fact that the number of probability functions $f^{(\xi)}$ that need to be stored are reduced from $|\mathcal{F}(\mathbb{L}) \times \Xi|$ to $|\Xi|$. This advantage also applies to the δ-GLMB UFS formulation.

The cardinality of a δ-GLMB UFS is obtained based on (20), i.e., $f_c(n) = \max_{(I,\xi)\in\mathcal{F}_n(\mathbb{L})\times\Xi} w^{(I,\xi)}$. It is clear that the cardinality of a δ-GLMB is a possibility function

This article has been accepted for publication in IEEE Transactions on Aerospace and Electronic Systems. This is the author's version which has not been fully edited and content may change prior to final publication. Citation information: DOI 10.1109/TAES.2022.3200022

with maximum equals one. The intensity measure of a δ-GLMB UFS can be obtained based on (22), i.e.,

$$\bar{v}(x) = \max_{\ell\in\mathbb{L}} \max_{(I,\xi)\in\mathcal{F}(\mathbb{L})\times\Xi} 1_I(\ell) w^{(I,\xi)} f^{(\xi)}(x,\ell).$$

The inner maximum can be seen as the intensity measure $\bar{v}^{(\ell)}(\cdot)$ of track ℓ. The set supremum of $\bar{v}^{(\ell)}(\cdot)$ leads to the possibility of existence of track ℓ, i.e., $r_1^{(\ell)} = \max_{(I,\xi)\in\mathcal{F}(\mathbb{L})\times\Xi} 1_I(\ell) w^{(I,\xi)}$.

As a special case of the GLMB UFS, the δ-GLMB UFS also solves the Bayes multi-target filter in a closed form. The derivation can be achieved following [7] but replacing the integrals and PDFs by supremums and respectively possibility functions.

B. Joint Prediction and Update

The formulation of the joint possibility δ-GLMB is shown in the following proposition and the proof is given in the Appendix.

PROPOSITION 4. *The posterior δ-GLMB possibility function can be derived as the function of the prior δ-GLMB as the following form*

$$\begin{aligned}\boldsymbol{\pi}(Z|\boldsymbol{X}) \propto \Delta(\boldsymbol{X}) &\max_{(I,\xi,I_+,\theta_+)} \omega^{(I,\xi)} \omega_Z^{(I,\xi,I_+,\theta_+)} \\ &\delta_{I_+}(\mathcal{L}(\boldsymbol{X}))\left[f_Z^{(\xi,\theta_+)}\right]^{\boldsymbol{X}},\end{aligned} \tag{31}$$

where

$$\begin{aligned}
\omega_Z^{(I,\xi,I_+,\theta_+)} &= 1_{\Theta(I_+)}(\theta_+)[r_{b,1}]^{\mathbb{B}\cap I_+}[r_{b,0}]^{\mathbb{B}-I_+} \\
&\quad\times\left[\eta_1^{(\xi)}\right]^{I\cap I_+}\left[\eta_0^{(\xi)}\right]^{I-I_+}\left[\eta_Z^{(\xi,\theta_+)}\right]^{I_+} \\
\eta_1^{(\xi)}(\ell) &= \sup_{x\in\mathbb{X}}\sup_{x'\in\mathbb{X}}\left[s_1(x',\ell)f(x|x',\ell)f^{(\xi)}(x',\ell)\right], \\
\eta_0^{(\xi)}(\ell) &= \sup_{x\in\mathbb{X}} s_0(x,\ell)f^{(\xi)}(x,\ell) \\
\eta_Z^{(\xi,\theta_+)}(\ell_+) &= \sup_{x\in\mathbb{X}} f^{(\xi)}(x,\ell_+)\psi_Z(x,\ell_+;\theta_+) \\
f_Z^{(\xi,\theta_+)}(x,\ell_+) &= \frac{f_+^{(\xi)}(x,\ell_+)\psi_Z(x,\ell_+;\theta_+)}{\eta_Z^{(\xi,\theta_+)}(\ell_+)}, \\
f_+^{(\xi)}(x,\ell_+) &= 1_{\mathbb{L}}(\ell_+)f_S^{(\xi)}(x,\ell_+) + (1-1_{\mathbb{L}}(\ell_+))f_B(x,\ell_+), \\
f_S^{(\xi)}(x,\ell_+) &= \frac{\sup_{x'\in\mathbb{X}}[s_1(x',\ell_+)f(x|x',\ell_+)f^{(\xi)}(x',\ell_+)]}{\eta_1^{(\xi)}(\ell_+)}.
\end{aligned}$$

The set of (I,ξ,I_+,θ_+) is generated using a Gibbs sampling method [31] with the stationary distribution $\omega_Z^{(I,\xi,I_+,\theta_+)}$, such that only valid children components with high weights are more likely to be sampled. The computational complexity of this approach is linear, which significantly reduces the computational load. Detailed implementation of the Gibbs sampler can be found in [31].

C. Linear GMM Representation

Under the assumption of linear multi-target dynamical model and observation model, and the distribution of measurement error and process noise variations are Gaussian. In addition, assume the single-target distribution and birth intensity are described by a GMM. The possibilistic expected value and variance of the predicted and updated GMM components are computed following the Kalman filter recursion [21].

For the linear Gaussian multi-target model, the transition function is Gaussian, $f(x_+|x,\ell) = \bar{\mathcal{N}}(x_+;Fx,Q)$, where F is the state transition matrix, and Q is the process noise variance. If the single target distribution $f^{(\xi)}(x,\ell)$ takes the form of GMM:

$$f^{(\xi)}(x,\ell) = \max_{1\le i\le N^{(\xi)}(\ell)} w_i^{(\xi)}\bar{\mathcal{N}}\big(x;\mu_i^{(\xi)}(\ell),S_i^{(\xi)}(\ell)\big),$$

and the birth intensity measure $f_B(x,\ell)$ is also a GMM, then, the predicted single target possibility function $f_+^{(\xi)}(x,\ell)$ is also a GMM

$$\begin{aligned}f_+^{(\xi)}(x,\ell) =& 1_{\mathbb{L}}(\ell)\max_{1\le i\le N^{(\xi)}(\ell)} w_i^{(\xi)}\bar{\mathcal{N}}\big(x;\mu_{S,i}^{(\xi)}(\ell),S_{S,i}^{(\xi)}(\ell)\big) \\ &+(1-1_{\mathbb{L}}(\ell))f_B(x,\ell),\end{aligned}$$

where the expected value and variance are given by

$$\begin{aligned}\mu_{S,i}^{(\xi)}(\ell) &= F\mu_i^{(\xi)}(\ell), \\ S_{S,i}^{(\xi)}(\ell) &= FS_i^{(\xi)}(\ell)F^T + Q.\end{aligned}$$

Supposing $s_1(x,\ell)$ and $s_0(x,\ell)$ are state and label independent, i.e., $s_1(x,\ell) = s_1$ and $s_0(x,\ell) = s_0$, the possibility of target survival and non-survival are given by $\eta_1^{(\xi)}(\ell) = s_1$ and $\eta_0^{(\xi)}(\ell) = s_0$, respectively.

For the linear Gaussian multi-target model, the likelihood function is Gaussian $g(z|x,\ell) = \bar{\mathcal{N}}(z;Hx,R)$, where H is the observation matrix and R is the observation noise variance. The possibility of a successful detection and detection failure are assumed to be state and label independent, i.e., $d_1(x,\ell) = d_1$ and $d_0(x,\ell) = d_0$. Given singe target distribution $f^{(\xi,\theta)}(\cdot|\ell)$ represented by a GMM

$$f^{(\xi,\theta)}(x|\ell) = \max_{1\le i\le N^{(\xi)}(\ell)} w_i^{(\xi)}(\ell)\bar{\mathcal{N}}\big(x;\mu_i^{(\xi)}(\ell),S_i^{(\xi)}(\ell)\big),$$

then, for an updated (ξ,θ), the posterior possibility function is also in the form of GMM, i.e.,

$$\begin{aligned}f^{(\xi,\theta)}(x,\ell|Z) &= \max_{1\le i\le N^{(\xi)}(\ell)} \frac{w_{Z,i}^{(\xi,\theta)}(\ell)}{\eta_Z^{(\xi,\theta)}(\ell)}\bar{\mathcal{N}}\big(x;\mu_i^{(\xi,\theta)}(\ell)S_i^{(\xi,\theta)}(\ell)\big) \\ \eta_Z^{(\xi,\theta)}(\ell) &= \max_{1\le i\le N^{(\xi)}(\ell)} w_{Z,i}^{(\xi,\theta)}(\ell),\end{aligned}$$

where

$$\begin{aligned}
w_{Z,i}^{(\xi,\theta)}(\ell) &= w_i^{(\xi)}\begin{cases}\frac{d_1\bar{\mathcal{N}}(z;\hat{z}_i^{(\xi)},S_{z,i}^{(\xi)}(\ell));\ell)}{\kappa(z_{\theta(\ell)})}, & \text{if } \theta(\ell)\neq 0 \\ d_0 & \text{if } \theta(\ell)=0\end{cases} \\
\mu_i^{(\xi,\theta)}(\ell) &= \begin{cases}\mu_i^{(\xi)} + K_i^{(\xi,\theta)}(\ell)(z-\hat{z}_i^{(\xi)}) & \text{if } \theta(\ell)\neq 0 \\ \mu_i^{(\xi)} & \text{if } \theta(\ell)=0\end{cases} \\
S_i^{(\xi,\theta)}(\ell) &= \begin{cases}[I-K_i^{(\xi,\theta)}(\ell)H]S_i^{(\xi)}(\ell) & \text{if } \theta(\ell)\neq 0 \\ S_i^{(\xi)}(\ell) & \text{if } \theta(\ell)=0\end{cases} \\
S_{z,i}^{(\xi)}(\ell) &= HS_i^{(\xi)}(\ell)H^T + R \\
K_i^{(\xi,\theta)}(\ell) &= S_i^{(\xi)}(\ell)H^T\big(S_{z,i}^{(\xi)}(\ell)\big)^{-1}.
\end{aligned}$$

D. Birth Model

There are two types of birth models that are generally used in labeled RFS filters. The first is to assume a fixed birth location [7, 8] within the sensor Field-of-View (FOV). The fixed birth location is particularly suitable for low signal to noise ratio applications since this assumption can effectively avoid generating too many birth tracks from false alarms. However, to establish the fixed birth location, we need some initial knowledge regarding the spatial distribution of newborn tracks, while this information may not be available in practice.

Alternatively, the measurement-driven birth model [9, 32, 33] generates birth distributions based on the measurements that have low association probability with existing tracks. In this paper, the association possibility $f_a(z)$ of each measurement z is calculated based on the maximum posterior weight $w^{(I,\xi,\theta)}$ including the track ℓ updated by z, which is given by

$$f_a(z) = \max_{(I,\xi)\in\mathcal{F}(\mathbb{L})\times\Xi} \max_{\theta\in\Theta} w^{(I,\xi,\theta)} 1_I(\theta^{-1}(z)).$$

If the association weight of z is lower than a threshold, then this measurement is employed to generate a newborn track. According to [18], the measurement-driven birth model in the OPM framework can be made uninformative when the state space is unbounded. The major drawback of this method is that it generates a large number of birth tracks, especially in the case of high clutter rate.

E. Multi-Target Estimation

Multi-target estimation can be seen as the maximum credibility given by the possibility δ-GLMB filter. Various types of multi-target estimators have been proposed for the probabilistic δ-GLMB filter, and two representative methods are the multi-Bernoulli estimator and the MAP cardinality estimator. Both estimators can be adapted to the proposed method. In this paper, the possibilistic MAP cardinality estimator is considered, where the cardinality estimate is given by

$$f_c(n) = \max_{(I,\xi)\in\mathcal{F}_n(\mathbb{L})\times\Xi} w^{(I,\xi)}.$$

The MAP cardinality $n^* = \arg\max_n f_c(n)$ is generated by the hypothesis with the highest posterior weight, i.e., $(I^*,\xi^*) = \arg\max_{I,\xi} w^{(I,\xi)}\delta_{n^*}(|I|)$. Then the states of all targets in I^* are extracted to represent the MAP multi-target state.

VII. Simulation

In this section, we compare the performance of the proposed method with the probabilistic δ-GLMB filter in two test scenarios. In the first case, the two multi-target trackers are applied to a general 2-dimensional multi-target tracking scenario. The second case considers a more challenging tracking scenario that employs a moving sensor with limited sensor FOV [18].

The state of a single target is modeled by a 4-dimensional vector $[x_1, x_2, \dot{x}_1, \dot{x}_2]$. Each target follows a linear motion model with a constant velocity in a 2-dimensional surveillance region S. The single target motion is governed by a linear Gaussian probability density $f_{k|k-1}(x_k|x_{k-1}) = \mathcal{N}\big(x_k; F_k x_{k-1}, Q_k\big)$. The state transition matrix F_k and process noise matrix Q_k are defined by

$$F = I_2 \otimes \begin{bmatrix} 1 & \Delta \\ 0 & 1 \end{bmatrix},\ Q = \sigma_p^2 I_2 \otimes \begin{bmatrix} \frac{\Delta^4}{4} & \frac{\Delta^3}{2} \\ \frac{\Delta^3}{2} & \frac{\Delta^4}{4} \end{bmatrix}, \quad (32)$$

where the time duration $\Delta = 1$ s, I_2 is a 2-dimensional identity matrix, σ_p is the Standard Deviation (STD) of the process noise, and $\otimes$ denotes the Kronecker product. The probability of target survival is a constant: $p_s = 0.99$.

The likelihood function is modeled by a Gaussian probability function $\mathcal{N}\big(z_k; H(x_k - x_{s,k}), R_k\big)$, where $x_{s,k}$ denotes the state of the sensor s at time k. The measurement function H and measurement noise R_k are given by

$$H = \begin{bmatrix} 1 & 0 & 0 & 0 \\ 0 & 0 & 1 & 0 \end{bmatrix},\ R_k = \sigma_r^2 I_2, \quad (33)$$

where $\sigma_r = 5$ m. The number of false alarms follows a Poisson distribution with a mean value λ_{fa}.

The true dynamical model and observation model are employed in the δ-GLMB filter. The possibility δ-GLMB filter, however, does not assume one has exact knowledge of the models. Hence, the single-target possibilistic dynamical model and likelihood function are described by a Gaussian possibility function $f_{k|k-1}(x_k|x_{k-1}) = \bar{\mathcal{N}}\big(x_k; F_k x_{k-1}, Q_k\big)$ and $\ell_k(z_k|x_k) = \bar{\mathcal{N}}\big(z_k; H(x_k - x_{s,k}), R_k\big)$, respectively. The possibility of survival s_1 is set to one and the possibility of non-survival is $s_0 = 0.01$. The possibility of successful detection and detection failure are defined by $d_1(x) = 1$ and $d_{0,k}(x) = 1 - p_{d,k}(x)$, respectively. The MAP cardinality estimator is employed to extract multi-target state.

Both methods are capped to 5000 components. The pruning threshold of the δ-GLMB filter is set to 1×10^{-4}, while the possibility δ-GLMB filter considers a larger threshold, i.e., 1×10^{-3} since possibilities is generally larger than probabilities. The merging approach in the possibility δ-GLMB filter is achieved based on the possibilistic Hellinger distance [18] with a threshold of 0.1. The δ-GLMB filter employs the Mahalanobis distance with a threshold of 4. Both methods are tested by 100 Monte Carlo (MC) trials. The Optimal Sub-Pattern Assignment (OSPA$^{(2)}$) distance metric [34] with a cutoff parameter $c = 100$ m, an order parameter $p = 2$, and a sliding time window of 10 is used to assess the tracking errors considering missed or false tracks.

A. Case A

This case evaluates the performance of the possibility δ-GLMB filter when the knowledge of the probability of detection is partially known. The scenario is restricted

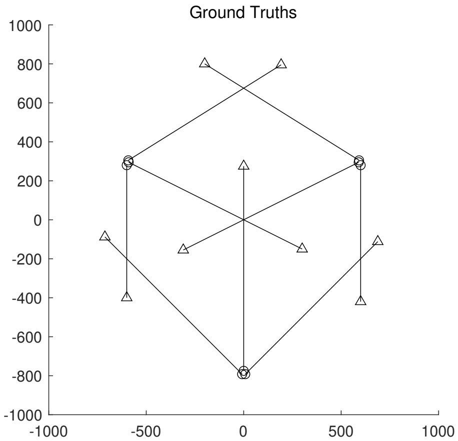

Fig. 1: Multi-target trajectories in the surveillance region, and each trajectory starts from a circle and ends with a triangle

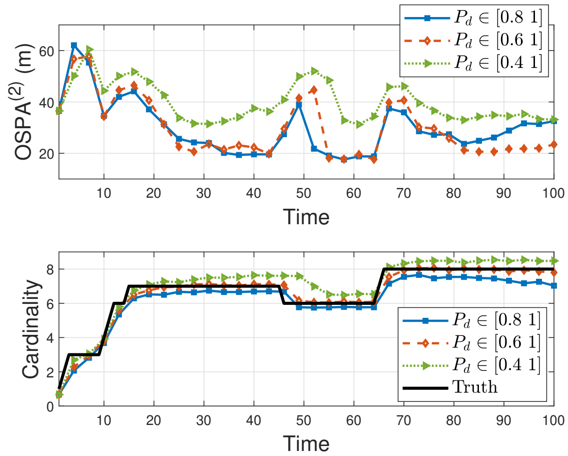

Fig. 2: Results of the possibility δ-GLMB filter using different P_d specifications

within a surveillance region $S = [-1000, 1000]$ m $\times$ $[-1000, 1000]$ m, and the sensor is fixed at the center of S with state $x_s = [0, 0, 0, 0]$. The total tracking period is discreted into 100 even time steps, and each duration is $\Delta = 1$ s. The target birth model is an LMB UFS represented by $\pi_B = \{(r_{b,0}^{(i)}, r_{b,1}^{(i)}, f_B^{(i)})\}_{i=1}^{3}$, where $r_{b,0}^{(i)} = 1$, $r_{b,1}^{(i)} = 0.01$, $f_B^{(i)}(x) = \bar{\mathcal{N}}(x; m_B^{(i)}, S_B^{(i)})$, and $m_B^{(1)} = [0, 0, -800, 0]^T$, $m_B^{(2)} = [600, 0, 300, 0]^T$, $m_B^{(3)} = [-600, 0, 300, 0]^T$, $S_B^{(i)} = \text{diag}([10, 10, 10, 10]^T)^2$. The existence possibility and non-existence possibility of birth targets are defined as $r_{b,1} = 0.01$ and $r_{b,0} = 1$, respectively. Assume we have the same information on the birth process in the two methods, the existence probability of newborn targets is defined as $r_B = 0.01$. This scenario assumes 9 targets born from 3 fixed locations. The trajectories of these targets are shown in Fig. 1.

Following the definition in [23], the detection probability is assumed as $P_d(x) = \exp\left[-(d/\beta)^4\right]$, where $d = ||x - x_s||$ and $\beta = 900$ m. The STD of the process noise is $\sigma_p = 0.1$ m/s. False alarms follow a Poisson distribution with an averaged number of $\lambda_{fa} = 10$ per frame. The possibility of false alarm is computed as $\kappa = \lambda_{fa}(2\pi\sigma_r^2)/V$, where V is the volume of the observation space and κ is a constant throughout the tracking [18].

This case assumes that the probability of detection P_d function is unavailable for analysis, and three P_d specifications, i.e., $P_d \in [0.4\ 1]$, $P_d \in [0.6\ 1]$, and $P_d \in [0.8\ 1]$, are tested to evaluate the performance of the proposed method in terms of different sensor profiles. The OSPA$^{(2)}$ distance and cardinality estimate of the method are shown in Fig. 2. Results show that the possibility δ-GLMB filter yields the most accurate state and cardinality estimates when using $P_d \in [0.6\ 1]$, indicating that the assumption of $P_d \in [0.6\ 1]$ properly captures the variations of the probability of detection of most targets. In addition, the filter employs a large bound of P_d, i.e., a smaller d_0 value, reacts more quickly to new target birth, while it also has a slow response to the disappearance of existing targets.

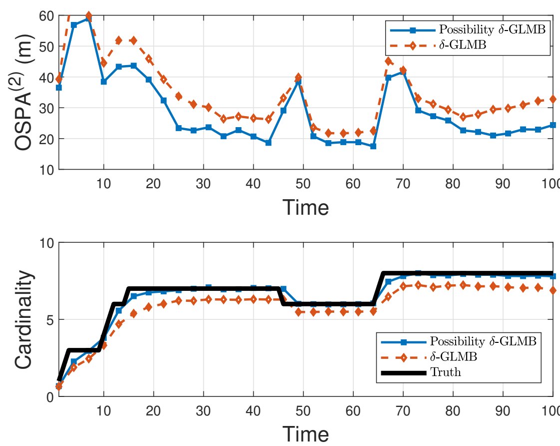

Fig. 3: Results of the possibility δ-GLMB filter and the δ-GLMB filter

To further validate the possibility δ-GLMB filter, the probabilistic δ-GLMB filter proposed in [19] is also tested using the same parameters and measurements. The probability of detection is assumed as unknown, and the δ-GLMB filter is able to adaptively learn P_d by modeling it using a beta distribution $\beta(\cdot; s, t)$. The initial value is set to $s = 8$ and $t = 2$, indicating that the initial guess of P_d is $\frac{s}{s+t} = 0.8$. The averaged OSPA$^{(2)}$ error and cardinality error of the two filters are shown in Fig. 3. In each subfigure, the blue solid curve represents the result of the possibility δ-GLMB filter using $P_d \in [0.6, 1]$, the red dashed curve shows the result of the δ-GLMB filter. Results show that the proposed method yields a better accuracy of state estimation and its cardinality is closer to the ground truth. The P_d of some targets change quickly in this case, especially when the target is relative far from the sensor. As the adaptive estimation method is not able to follow the rapid variation of P_d, the δ-GLMB filter may yield missed detections, such that leading to inaccurate state estimation.

B. Case B

In this case study, a moving sensor with limited FOV is employed to monitor a compact region $S = [0, 1000]$ m $\times$ $[0, 1000]$ m. The initial state x_s of the sensor is randomly generated, where the position components are uniformly distributed within S and the velocity components have a constant magnitude 50 m/s. The sensor will turn an angle $\pm 90^\circ$ if it reaches the bound of S, and the velocity of the sensor is subject to a rotation by a normally distributed random angle with mean 0 rad and variance 0.05 rad. The total tracking period is 200 time steps with duration of $\Delta = 1$ s. The STD of the process noise is $\sigma_p = 0.01$ m/s^2.

The number of new targets follows a Poisson distribution with $\lambda_b = 0.3$, and the new target birth is only allowed before time $k = 30$. The initial position of new targets is uniformly distributed within S, and the initial velocity is generated based on the possibility function based on a zero mean Gaussian distribution with STD $\sigma_v = 1$ m/s. The measurement-driven birth model is employed to conduct new target birth, where the velocity components are randomly generated based on the zero mean Gaussian distribution with STD $\sigma_v = 1$ m/s. The existence possibility and non-existence possibility of birth targets are defined as $r_{b,1} = 0.01$ and $r_{b,0} = 1$, respectively. Assuming we have the same information on birth process, the existence probability of birth targets is defined as $r_B = 0.01$ for the δ-GLMB filter. The probability of detection is time-varying, which is calculated based on $p_{d,k}(x) = \bar{\mathcal{N}}(x; x_{s,k}, \sigma_s^2 I_2)$ with $\sigma_s = 150$ describing the sensor's detection capability. As opposed to the previous case, the state-dependent probability of detection $p_{d,k}(x)$ is used directly by both methods in this scenario. The number of false alarms are Poisson distributed with $\lambda_{fa} = 1$, and they are generated from $\mathcal{N}(Hx_{s,k}, \sigma_s^2 I_2)$. The possibility of false alarm is calculated as $\kappa(z) = \lambda_{fa}(2\pi\sigma_r^2)\bar{\mathcal{N}}(z, Hx_{s,k}, \sigma_s^2 I_2)/V$, where the volume of the observation space is $V = 2\pi\sigma_s^2$.

Fig. 4 shows an example of the multi-target tracking scenario at time $k = \{20, 40, 60, 80\}$. The trajectory of the sensor is shown as the blue curve with circles to represent its position at each epoch. The triangle and the square denote the position of the sensor at the start point and the time instance k, respectively. The red dotted ellipse represents the 1-σ bound of the sensor FOV, and the red cross represents the measurements at time k. It can be seen that a target might be outside the sensor FOV over a long time period, which introduces an additional difficulty to maintain custody of its identity.

The top panel in Fig. 5 shows the averaged OSPA$^{(2)}$ distance of the two methods using the MAP cardinality estimator over 100 MC tests. It is clear that the proposed method yields a smaller OSPA$^{(2)}$ distance than the δ-GLMB filter after time $k = 50$. The bottom panel in Fig. 5 shows the cardinality estimation results. The ground truth is an averaged value over 100 MC runs, and it gradually decreases after time $k = 30$ since some targets move out of the surveillance region over time. The possibility δ-GLMB filter outperforms the δ-GLMB filter, and it can eventually approximate the ground truth. As the sensor has a limited FOV, the detection probability of some targets that around the bound of the FOV is very low. Thus, the standard δ-GLMB filter may fail to establish the existence of new targets when both their existence probability and detection probability are extremely low. However, the possibility δ-GLMB filter is able to react more quickly to new target birth when we have little information about the birth and detection process. This result demonstrates that the proposed method can better deal with the uncertainty in the number of targets, and

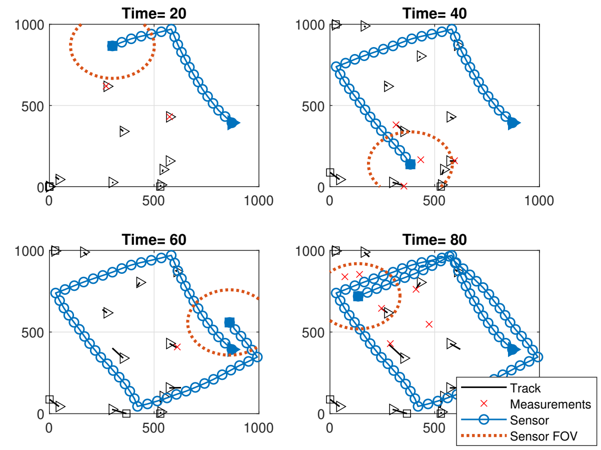

Fig. 4: An example of multi-target and moving sensor trajectories at time $k = \{20, 40, 60, 80\}$.

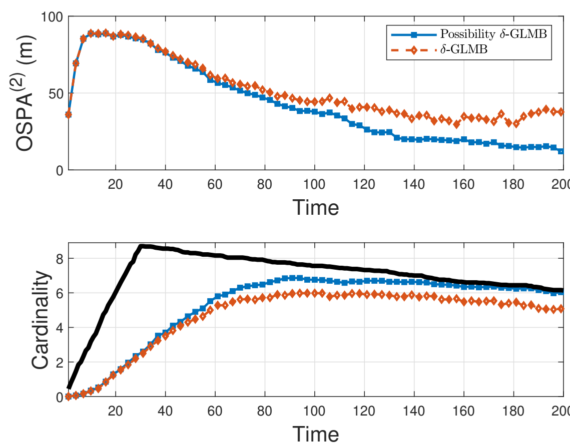

Fig. 5: Results of the possibility δ-GLMB filter and the δ-GLMB filter

it provides a more robust solution to maintain custody of multiple targets in the absence of initial knowledge of their existence.

VIII. Conclusion

The contribution of this paper is a possibility Generalized Labeled Multi-Bernoulli (GLMB) filter based on the notion of Outer Probability Measures (OPMs). The major advantage of this approach is the capability to properly account for epistemic uncertainty that comes from ignorance or partial knowledge of a multi-target tracking system, such as the absence of perfect information about the sensor profiles and the number of newborn targets.

Similar to the probabilistic GLMB random finite set, the family of GLMB Uncertain Finite Set (UFS) possibility functions are conjugate priors that are closed under the multi-object Chapman-Kolmogorov equation. The prediction and update recursion of the possibility GLMB filter has a similar form as the standard probabilistic GLMB filter but with supermums and possibility functions instead of integrals and probability density functions, respectively. The feasibility of the possibility δ-GLMB filter is validated using two simulated multi-target tracking scenarios. The first is a general two-dimensional tracking case and the second is a more challenging case that considers a moving sensor with a limited FOV. Compared to the standard δ-GLMB filter, the proposed method yields more accurate state and cardinality estimation in the situation of imperfect information of some aspects of the system.

Future research will study efficient approximations of the possibility δ-GLMB filter, such as the possibility LMB filter and the possibility marginalized GLMB filter. It is also of interest to study multi-sensor multi-target tracking algorithms based on the GLMB UFS for robust information fusion in the absence of statistical information of data sets.

Acknowledgments

This work was funded by Science and Technology on Space Intelligent Control Laboratory, No.HTKJ2021KL502017.

APPENDIX

Proof of the cardinality function of multi-Bernoulli UFS:

We first prove the supremum of a multi-Bernoulli possibility function π is equal to one, i.e., $\max_{X\in\mathbb{X}} \pi(X) = 1$.

$$\begin{aligned}
&\sup_{X\in\mathbb{X}} \pi(X)\\
&= \max\left\{\pi(\cup_{i=1}^{n}\emptyset), \sup_{\{x_1,\dots,x_n\}\in\mathbb{X}} \left[\pi(\{x_1,\dots,x_n\})\right]\right\}\\
&= \max\left\{\prod_{i=1}^{m} r_0^{(i)}, \max_{1\le n\le m}\left[\prod_{i=1}^{m} r_0^{(i)} \max_{\substack{1\le i_1,\neq\dots,\\ \neq i_n\le m}}\left[\prod_{j=1}^{n}\frac{r_1^{(i_j)}}{r_0^{(i_j)}}\right.\right.\right.\\
&\qquad\left.\left.\left.\times \sup_{x_j\in\mathbb{X}} f^{(i_j)}(x_j)\right]\right]\right\}\\
&= \max\left\{\prod_{i=1}^{m} r_0^{(i)}, \max_{1\le n\le m}\left[\prod_{i=1}^{m} r_0^{(i)} \max_{\substack{1\le i_1,\neq\dots,\\ \neq i_n\le m}}\prod_{j=1}^{n}\frac{r_1^{(i_j)}}{r_0^{(i_j)}}\right]\right\}.
\end{aligned} \tag{34}$$

Deriving the supremum of $\pi(X)$ depends on the following two conditions.

(1) If $\prod_{i=1}^{m} r_0^{(i)} = 1$, the solution of (34) can be determined as $\sup_{X\in\mathbb{X}}\{\pi(X)\} = \max\prod_{i=1}^{m} r_0^{(i)} = 1$. In this case, we have no evidence to reject that all the elements are empty: $X^{(i)} = \emptyset$.

(2) In the case of $\prod_{i=1}^{m} r_0^{(i)} \neq 1$, we can rewrite the inner maximum in (34) as the following form

$$\max_{1\le i_1,\neq\dots,\neq i_n\le m}\prod_{j=1}^{n}\frac{r_1^{(i_j)}}{r_0^{(i_j)}} = \max_{1\le n\le m}\prod_{j\in\{i_1,\dots,i_n\}}\frac{r_1^{(j)}}{r_0^{(j)}}. \tag{35}$$

Suppose there is a non-empty set $\{j_1,\dots,j_n\}$, where for any $j\in\{j_1,\dots,j_n\}$, $r_1^{(j)} = 1$ and $r_0^{(j)} \le 1$. For any $j'\notin\{j_1,\dots,j_n\}$, it is obvious that $r_0^{(j')} = 1$ and $r_1^{(j')} \le 1$ due to normalization: $\max\{r_0^{(j')}, r_1^{(j')}\} = 1$. Hence, (35) can be simplified as below

$$\max_{1\le n\le m}\prod_{j\in\{i_1,\dots,i_n\}}\frac{r_1^{(j)}}{r_0^{(j)}} = \prod_{j\in\{j_1,\dots,j_n\}}\frac{r_1^{(j)}}{r_0^{(j)}}, \tag{36}$$

because only the terms $j\in\{j_1,\dots,j_n\}$ can yield $\frac{r_1^{(j)}}{r_0^{(j)}} \ge 1$, involving any $j'\notin\{j_1,\dots,j_n\}$ in the product can only lower its value.

Substituting (36) into (34), we have

$$\begin{aligned}
&\max_{1\le n\le m}\left[\prod_{i=1}^{m} r_0^{(i)} \max_{1\le i_1,\neq\dots,\neq i_n\le m}\prod_{j=1}^{n}\frac{r_1^{(i_j)}}{r_0^{(i_j)}}\right]\\
&= \prod_{i\in\{1,\dots,m\}} r_0^{(i)} \prod_{j\in\{j_1,\dots,j_n\}}\frac{r_1^{(j)}}{r_0^{(j)}}\\
&= \prod_{i\in\{1,\dots,m\}/\{j_1,\dots,j_n\}} r_0^{(i)} \prod_{j\in\{j_1,\dots,j_n\}} r_1^{(j)} = 1,
\end{aligned}$$

because all the $r_0^{(i)}$ and $r_1^{(j)}$ are equal to one.

Based on the above two cases, we can conclude that $\sup_{X\in\mathbb{X}}\pi(X) = 1$ holds true.

Then, the maximum of the cardinality function of the Bernoulli UFS is given by

$$\begin{aligned}
&\max_{n\ge 0} f_c(n)\\
&= \max_{1\le n\le m}\left[\prod_{i=1}^{m} r_0^{(i)}, \prod_{i=1}^{m} r_0^{(i)} \max_{1\le i_1,\neq\dots,\neq i_n\le m}\prod_{j=1}^{n}\frac{r_1^{(i_j)}}{r_0^{(i_j)}}\right]\\
&= 1.
\end{aligned}$$

■

The following two Lemmas can be used to simplify the distinct label indicator $\Delta(\boldsymbol{X})$ from the labeled UFS expressions, which are frequently employed to evaluate the labeled UFS.

Lemma 1

Given a symmetric function $f : \mathbb{L}^n \to \mathbb{R}$, then

$$\begin{aligned}\max_{(\ell_1,\ldots,\ell_n)\in\mathbb{L}^n} &\delta_n(|\{\ell_1,\ldots,\ell_n\}|)f(\ell_1,\ldots,\ell_n)\\ &= \max_{\{\ell_1,\ldots,\ell_n\}\in\mathcal{F}_n(\mathbb{L})} f(\ell_1,\ldots,\ell_n)\end{aligned} \tag{37}$$

Lemma 2

For function $f : \mathbb{X}\times\mathbb{L} \to \mathbb{R}$ and $\omega : \mathcal{F}(\mathbb{L}) \to \mathbb{R}$, we have

$$\sup_{\boldsymbol{X}\in\mathbb{X}\times\mathbb{L}} \left[\Delta(\boldsymbol{X})\omega(\mathcal{L}(\boldsymbol{X}))f^{\boldsymbol{X}}\right] = \max_{L\subseteq\mathbb{L}} \omega(L)\left[\sup_{x\in\mathbb{X}} f(x,\cdot)\right]^L. \tag{38}$$

Proof of Lemma 1:

Note the distinction between $\mathbb{L}^n$ and $\mathcal{F}_n(\mathbb{L})$. The former is the $n!$ permutations of labels with cardinality equals n, while the later is all the finite subsets of labels with cardinality equals n. Due to the distinct label indicator $\delta_n(|\{\ell_1,\ldots,\ell_n\}|)$, the maximum in the LHS of (37) is a maximum over $n!$ permutations of $(\ell_1,\ldots,\ell_n)$ in $\mathbb{L}^n$ with distinct labels. As f is symmetric, the values of $f(\ell_1,\ldots,\ell_n)$ for all permutations of $(\ell_1,\ldots,\ell_n)$ are identical. Therefore, Lemma 1 holds true.

Lemma 1 is different from Lemma 12 in [7], where the sum over indices $\mathbb{L}^n$ with distinct labels equals $n!$ permutations of $\{\ell_1,\ldots,\ell_n\}\in\mathcal{F}_n(\mathbb{L})$, Lemma 1 indicates that the maximum functional value of all permutations is the same as the maximum functional value of the set $\{\ell_1,\ldots,\ell_n\}$.

■

Proof of Lemma 2:

According to (11), (38) can be rewritten as

$$\begin{aligned}&\sup_{\boldsymbol{X}\in\mathbb{X}\times\mathbb{L}} \left[\Delta(\boldsymbol{X})\omega(\mathcal{L}(\boldsymbol{X}))f^{\boldsymbol{X}}\right]\\
&= \max_{n\geq 0}\Bigg[\max_{(\ell_1,\ldots,\ell_n)\in\mathbb{L}^n} \delta_n(|\{\ell_1,\ldots,\ell_n\}|)\omega(\{\ell_1,\ldots,\ell_n\})\\
&\qquad\times\left[\sup_{\{x_1,\ldots,x_i\}\in\mathbb{X}^i}\prod_{i=1}^n f(x_i,\ell_i)\right]\Bigg]\\
&= \max_{n\geq 0}\left[\max_{\{\ell_1,\ldots,\ell_n\}\in\mathcal{F}_n(\mathbb{L})} \omega(\{\ell_1,\ldots,\ell_n\})\prod_{i=1}^n\sup_{x_i\in\mathbb{X}} f(x_i,\ell_i)\right]\\
&= \max_{L\subseteq\mathbb{L}}\omega(L)\left[\sup_{x\in\mathbb{X}} f(x,\cdot)\right]^L,\end{aligned}$$

where the distinct label indicator is removed according to Lemma 1. ■

Proof of the cardinality function and intensity measure of GLMB UFS:

Given an UFS $\boldsymbol{X} = \{(x_1,\ell_1),\ldots,(x_n,\ell_n)\}$, the distinct label indicator is expressed as $\Delta(\boldsymbol{X}) = \delta_n(|\{\ell_1,\ldots,\ell_n\}|)$. Based on proposition 1 and Lemma 1, the cardinality function of a GLMB UFS is given by

$$\begin{aligned}&f_c(n)\\
&= \max_{(\ell_1,\ldots,\ell_n)\in\mathbb{L}^n} \delta_n(|\{\ell_1,\ldots,\ell_n\}|)\max_{o\in\mathbb{O}} w^{(o)}(\{\ell_1,\ldots,\ell_n\})\\
&\times\left[\prod_{i=1}^n\sup_{x_i\in\mathbb{X}} f^{(o)}(x_i,\ell_i)\right]\\
&= \max_{o\in\mathbb{O}}\max_{(\ell_1,\ldots,\ell_n)\in\mathbb{L}^n} \delta_n(|\{\ell_1,\ldots,\ell_n\}|)w^{(o)}(\{\ell_1,\ldots,\ell_n\})\\
&= \max_{o\in\mathbb{O}}\max_{L\in\mathcal{F}_n(\mathbb{L})} w^{(o)}(L).\end{aligned}$$

According to (10), the intensity measure (5) of an UFS can be rewritten as the function of the labeled possibility function $\boldsymbol{\pi}$

$$\begin{aligned}&\bar{v}(x)\\
&= \max_{n\geq 0}\sup_{(x_1,\ldots,x_n)\in\mathbb{X}^n}\max_{(\ell,\ell_1,\ldots,\ell_n)\in\mathbb{L}^{n+1}} \boldsymbol{\pi}(\{x,\ell\}\\
&\quad\cup\{(x_1,\ell_1),\ldots,(x_n,\ell_n)\})\\
&= \max_{n\geq 0}\sup_{(x_1,\ldots,x_n)\in\mathbb{X}^n}\max_{(\ell,\ell_1,\ldots,\ell_n)\in\mathbb{L}^{n+1}} \delta_{n+1}(|\{\ell,\ell_1,\ldots,\ell_n\}|)\\
&\quad\times\max_{o\in\mathbb{O}} w^{(o)}(\{\ell,\ell_1,\ldots,\ell_n\})f^{(o)}(x,\ell)\left[f^{(o)}\right]^{\boldsymbol{X}}\\
&= \max_{n\geq 0}\max_{\ell\in\mathbb{L}}\max_{(\ell_1,\ldots,\ell_n)\in\mathbb{L}^n} \delta_n(|\{\ell_1,\ldots,\ell_n\}|)\\
&\quad\times(1-1_{\{\ell_1,\ldots,\ell_n\}}(\ell))\max_{o\in\mathbb{O}} w^{(o)}(\{\ell,\ell_1,\ldots,\ell_n\})f^{(o)}(x,\ell)\\
&= \max_{o\in\mathbb{O}}\max_{\ell\in\mathbb{L}}\max_{n\geq 0}\max_{I\in\mathcal{F}_n(\mathbb{L})}(1-1_I(\ell))w^{(o)}(\{\ell\}\cup I)f^{(o)}(x,\ell)\\
&= \max_{o\in\mathbb{O}}\max_{\ell\in\mathbb{L}} f^{(o)}(x,\ell)\max_{L\subseteq\mathbb{L}}1_L(\ell)w^{(o)}(L),\end{aligned}$$

where $I = \{\ell_1,\ldots,\ell_n\}$ and $L = \{\ell\}\cup I$. Since all permutations of $\{\ell,\ell_1,\ldots,\ell_n\}$ yield the same value of $w^{(o)}(\{\ell,\ell_1,\ldots,\ell_n\})$, the distinct label indicator $\delta_n(|\{\ell_1,\ldots,\ell_n\}|)$ is eliminated by applying Lemma 1.

■

Proof of Proposition 2:

According to (18), the multi-target likelihood function is the superposition of the possibility functions of detection and false alarms. Substituting (16) and (17) into (18) yields the following explicit expression of the multi-target likelihood function

$$\begin{aligned}g(Z|\boldsymbol{X}) =&\pi_F(Z)\max_{W\subseteq Z}\left[\frac{\pi_D(W|\boldsymbol{X})}{\pi_F(W)}\right]\\
=&\kappa^Z\prod_{i=1}^{|\boldsymbol{X}|}d_0(\boldsymbol{x}_i)\max_\theta\delta_{\theta^{-1}(\{0:|Z|\})}(\mathcal{L}(\boldsymbol{X}))\\
&\times\prod_{i:\theta(i)>0}\frac{d_1(\boldsymbol{x}_i)g(z_{\theta(\ell)}|\boldsymbol{x}_i)}{d_0(\boldsymbol{x}_i)\kappa(z_{\theta(i)})}.\end{aligned}$$

Assuming the labels are distinct, the above equation can be rewritten as a form of GLMB UFS function, i.e.,

$$\begin{aligned}g(Z|\boldsymbol{X}) &= \kappa^Z\prod_{i=1}^{|\boldsymbol{X}|}d_0(\boldsymbol{x}_i)\max_\theta\prod_{i:\theta(i)>0}\frac{d_1(\boldsymbol{x}_i)g(z_{\theta(\ell)}|\boldsymbol{x}_i)}{d_0(\boldsymbol{x}_i)\kappa(z_{\theta(i)})}\\
&= \kappa^Z\max_{\theta\in\Theta}\delta_{\theta^{-1}(\{0:|Z|\})}(\mathcal{L}(\boldsymbol{X}))\left[\psi_Z(\cdot;\theta)\right]^{\boldsymbol{X}}.\end{aligned}$$

The product of the multi-target likelihood function $g(\cdot|\cdot)$ and the prior GLMB function $\boldsymbol{\pi}(\cdot)$ yields a similar form as that of the probabilistic version in [7]. Therefore, the posterior multi-target UFS can be derived by dividing $g(\cdot|\cdot)\boldsymbol{\pi}(\cdot)$ by its supremum following the derivation in [7]. ■

The proof of proposition 3 can be achieved by using Lemma 2 and following the derivation of probabilistic GLMB recursions in [7].

Proof of proposition 4:
The weight $w^{(I_+,\xi,\theta_+)}(Z)$ of the posterior δ-GLMB can be expressed as

$$\begin{aligned}
&w^{(I_+,\xi,\theta_+)}(Z)\\
&=\delta_{\theta_+^{-1}(\{0:|Z|\})}(I_+)\left[\eta_Z^{(\xi,\theta_+)}\right]^{I_+}w_+^{(I_+,\xi)}\\
&=\delta_{\theta_+^{-1}(\{0:|Z|\})}(I_+)\left[\eta_Z^{(\xi,\theta_+)}\right]^{I_+}w_B(\mathbb{B}\cap I_+)w_S^{(\xi)}(\mathbb{L}\cap I_+)\\
&=1_{\Theta_+(I_+)}(\theta_+)\Big[1_{\mathcal{F}(\mathbb{B})}(\mathbb{B}\cap I_+)r_{b,1}^{\mathbb{B}\cap I_+}r_{b,0}^{\mathbb{B}-\mathbb{B}\cap I_+}\Big]\\
&\quad\times\Big[\max_{I\subseteq\mathcal{F}(\mathbb{L})}1_{\mathcal{F}(I)}(\mathbb{L}\cap I_+)\left[\eta_1^{(\xi)}\right]^{\mathbb{L}\cap I_+}\\
&\quad\times\left[\eta_0^{(\xi)}\right]^{I-\mathbb{L}\cap I_+}w^{(I,\xi)}\Big]\left[\eta_Z^{(\xi,\theta_+)}\right]^{I_+}\\
&=1_{\Theta_+(I_+)}(\theta_+)r_{b,1}^{\mathbb{B}\cap I_+}r_{b,0}^{\mathbb{B}-\mathbb{B}\cap I_+}\Big[\max_{I\subseteq\mathcal{F}(\mathbb{L})}\left[\eta_1^{(\xi)}\right]^{I\cap I_+}\\
&\quad\times\left[\eta_0^{(\xi)}\right]^{I-\mathbb{L}\cap I_+}w^{(I,\xi)}\Big]\left[\eta_Z^{(\xi,\theta_+)}\right]^{I_+}\\
&=\max_{I\subseteq\mathcal{F}(\mathbb{L})}w^{(I,\xi)}\omega_Z^{(I,\xi,I_+,\theta_+)}
\end{aligned}$$

■

REFERENCES

[1] D. Reid, "An algorithm for tracking multiple targets," *IEEE transactions on Automatic Control*, vol. 24, no. 6, pp. 843–854, 1979.

[2] T. Fortmann, Y. Bar-Shalom, and M. Scheffe, "Sonar tracking of multiple targets using joint probabilistic data association," *IEEE journal of Oceanic Engineering*, vol. 8, no. 3, pp. 173–184, 1983.

[3] R. P. Mahler, *Statistical multisource-multitarget information fusion*. Artech House, Inc., 2007.

[4] R. Mahler, "PHD filters of higher order in target number," *IEEE Transactions on Aerospace and Electronic Systems*, vol. 43, no. 4, 2007.

[5] R. P. Mahler, B.-T. Vo, and B.-N. Vo, "CPHD filtering with unknown clutter rate and detection profile," *IEEE Transactions on Signal Processing*, vol. 59, no. 8, pp. 3497–3513, 2011.

[6] B.-T. Vo, B.-N. Vo, and A. Cantoni, "The cardinality balanced multi-target multi-Bernoulli filter and its implementations," *IEEE Transactions on Signal Processing*, vol. 57, no. 2, pp. 409–423, 2009.

[7] B.-T. Vo and B.-N. Vo, "Labeled random finite sets and multi-object conjugate priors," *IEEE Transactions on Signal Processing*, vol. 61, no. 13, pp. 3460–3475, 2013.

[8] B.-N. Vo, B.-T. Vo, and D. Phung, "Labeled random finite sets and the Bayes multi-target tracking filter," *IEEE Transactions on Signal Processing*, vol. 62, no. 24, pp. 6554–6567, 2014.

[9] S. Reuter, B.-T. Vo, B.-N. Vo, and K. Dietmayer, "The labeled multi-Bernoulli filter," *IEEE Transactions on Signal Processing*, vol. 62, no. 12, pp. 3246–3260, 2014.

[10] C. Fantacci and F. Papi, "Scalable multisensor multitarget tracking using the marginalized δ-GLMB density," *IEEE Signal Processing Letters*, vol. 23, no. 6, pp. 863–867, 2016.

[11] F. Papi, B.-N. Vo, B.-T. Vo, C. Fantacci, and M. Beard, "Generalized labeled multi-Bernoulli approximation of multi-object densities," *IEEE transactions on signal processing*, vol. 63, no. 20, pp. 5487–5497, 2015.

[12] H. Cai, S. Gehly, Y. Yang, R. Hoseinnezhad, R. Norman, and K. Zhang, "Multisensor tasking using analytical Rényi divergence in labeled multi-bernoulli filtering," *Journal of Guidance, Control, and Dynamics*, vol. 42, no. 9, pp. 2078–2085, 2019.

[13] S. Gehly, "Estimation of geosynchronous space objects using finite set statistics filtering methods," Ph.D. dissertation, University of Colorado at Boulder, 2016.

[14] M. Beard, B.-T. Vo, B.-N. Vo, and S. Arulampalam, "Void probabilities and Cauchy–Schwarz divergence for generalized labeled multi-Bernoulli models," *IEEE Transactions on Signal Processing*, vol. 65, no. 19, pp. 5047–5061, 2017.

[15] B.-N. Vo, B.-T. Vo, and M. Beard, "Multi-sensor multi-object tracking with the generalized labeled multi-Bernoulli filter," *IEEE Transactions on Signal Processing*, vol. 67, no. 23, pp. 5952–5967, 2019.

[16] C. Fantacci, B.-N. Vo, B.-T. Vo, G. Battistelli, and L. Chisci, "Robust fusion for multisensor multi-object tracking," *IEEE Signal Processing Letters*, vol. 25, no. 5, pp. 640–644, 2018.

[17] E. Delande, J. Houssineau, and M. Jah, "A new representation of uncertainty for data fusion in SSA detection and tracking problems," in *2018 21st International Conference on Information Fusion (FUSION)*. IEEE, 2018, pp. 1–8.

[18] J. Houssineau, "A linear algorithm for multi-target tracking in the context of possibility theory," *IEEE Transactions on Signal Processing*, vol. 69, pp. 2740–2751, 2021.

[19] Y. G. Punchihewa, B.-T. Vo, B.-N. Vo, and D. Y. Kim, "Multiple object tracking in unknown backgrounds with labeled random finite sets," *IEEE Transactions on Signal Processing*, vol. 66, no. 11, pp. 3040–3055, 2018.

[20] C.-T. Do, T. T. D. Nguyen, and H. Van Nguyen, "Robust multi-sensor generalized labeled multi-Bernoulli filter," *Signal Processing*, vol. 192, p. 108368, 2022.

[21] J. Houssineau and A. N. Bishop, "Smoothing and filtering with a class of outer measures," *SIAM/ASA Journal on Uncertainty Quantification*, vol. 6, no. 2, pp. 845–866, 2018.

[22] E. Delande, J. Houssineau, J. Franco, C. Frueh, D. Clark, and M. Jah, "A new multi-target tracking algorithm for a large number of orbiting objects," *Advances in Space Research*, vol. 64, no. 3, pp. 645–667, 2019.

[23] B. Ristic, J. Houssineau, and S. Arulampalam, "Target tracking in the framework of possibility theory: The possibilistic Bernoulli filter," *Information Fusion*, vol. 62, pp. 81–88, 2020.

[24] D. Dubois and H. Prade, "Possibility theory and its applications: Where do we stand?" in *Springer handbook of computational intelligence*. Springer, 2015, pp. 31–60.

[25] ——, "Fuzzy sets in approximate reasoning, part 1: Inference with possibility distributions," *Fuzzy sets and systems*, vol. 40, no. 1, pp. 143–202, 1991.

[26] ——, "Representation and combination of uncertainty with belief functions and possibility measures," *Computational intelligence*, vol. 4, no. 3, pp. 244–264, 1988.

[27] D. Dubois, H. T. Nguyen, and H. Prade, "Possibility theory, probability and fuzzy sets misunderstandings, bridges and gaps," in *Fundamentals of fuzzy sets*. Springer, 2000, pp. 343–438.

[28] H. Cai, I. Hussein, and M. Jah, "Possibilistic admissible region using outer probability measure theory," *Acta Astronautica*, 2020.

[29] K. J. DeMars and M. K. Jah, "Probabilistic initial orbit determination using Gaussian mixture models," *Journal of Guidance, Control, and Dynamics*, vol. 36, no. 5, pp. 1324–1335, 2013.

[30] J. Houssineau, J. Zeng, and A. Jasra, "Uncertainty modelling and computational aspects of data association," *Statistics and Computing*, vol. 31, no. 5, pp. 1–19, 2021.

[31] B.-N. Vo, B.-T. Vo, and H. G. Hoang, "An efficient implementation of the generalized labeled multi-Bernoulli filter," *IEEE Transactions on Signal Processing*, vol. 65, no. 8, pp. 1975–1987, 2017.

[32] H. Cai, S. Gehly, Y. Yang, and K. Zhang, "Modeling birth for the labeled multi-Bernoulli filter using a boundary-value approach," *Journal of Guidance, Control, and Dynamics*, vol. 43, no. 1, pp. 162–169, 2020.

[33] B. A. Jones, "CPHD filter birth modeling using the probabilistic admissible region," *IEEE Transactions on Aerospace and Electronic Systems*, vol. 54, no. 3, pp. 1456–1469, 2018.

[34] M. Beard, B. T. Vo, and B.-N. Vo, "A solution for large-scale multi-object tracking," *IEEE Transactions on Signal Processing*, vol. 68, pp. 2754–2769, 2020.